Available online at www.sciencedirect.com
ScienceDirect
Geomorphology 100 (2008) 377–400
GEOMORPHOLOGY
www.elsevier.com/locate/geomorph

Alexander the Great's tombolos at Tyre and Alexandria, eastern Mediterranean

N. Marriner [a,*], J.P. Goiran [b], C. Morhange [a]

[a] CNRS CEREGE UMR 6635, Université Aix-Marseille, Europôle de l'Arbois, BP 80, 13545 Aix-en-Provence cedex 04, France
[b] CNRS MOM Archéorient UMR 5133, 5/7 rue Raulin, 69365 Lyon cedex 07, France

Received 25 July 2007; received in revised form 10 January 2008; accepted 11 January 2008
Available online 2 February 2008

Abstract

Tyre and Alexandria's coastlines are today characterised by wave-dominated tombolos, peculiar sand isthmuses that link former islands to the adjacent continent. Paradoxically, despite a long history of inquiry into spit and barrier formation, understanding of the dynamics and sedimentary history of tombolos over the Holocene timescale is poor. At Tyre and Alexandria we demonstrate that these rare coastal features are the heritage of a long history of natural morphodynamic forcing and human impacts. In 332 BC, following a protracted seven-month siege of the city, Alexander the Great's engineers cleverly exploited a shallow sublittoral sand bank to seize the island fortress; Tyre's causeway served as a prototype for Alexandria's Heptastadium built a few months later. We report stratigraphic and geomorphological data from the two sand spits, proposing a chronostratigraphic model of tombolo evolution.

Keywords: Tombolo; Spit; Tyre; Alexandria; Mediterranean; Holocene

1. Introduction

The term tombolo is used to define a spit of sand or shingle linking an island to the adjacent coast. Despite a long history of inquiry (Gulliver, 1896, 1899; Johnson, 1919; Escoffier, 1954; Guilcher, 1958), the literature has traditionally focused upon form-process aspects of their geomorphology with very little attention being paid to the salients' sedimentary history. Whilst the origins of spits and barrier islands have been the subject of significant scientific debate, notably with the rich North American literature (see Davis, 1994; Stapor and Stone, 2004; Stone et al., 2004; Schwartz and Birkemeier, 2004; Otvos and Giardino, 2004; Gardner et al., 2005; Simms et al., 2006), papers discussing tombolo evolution – their stratigraphic architecture and stages of accretion – are few and far between. The meagre corpus of recent literature has tended to concentrate on: (1) the role of contemporary processes operating around tombolos (Hine, 1979; Dally and Pope, 1986; Silvester and Hsu, 1993; Flinn, 1997; Courtaud, 2000; Browder and McNinch, 2006); (2) establishing a typology of shoreline salients and tombolos (Zenkovich, 1967; Sanderson and Eliot, 1996); and (3) modelling the geometrical relationships of these depositional forms relative to the breakwater island (Ming and Chiew, 2000). Although the use of detached breakwaters in shoreline protection has renewed interest in salient accretion, understanding of the dynamics and sedimentary history of these forms on longer centennial and millennial timescales remains poor (Clemmensen et al., 2001).

The processes governing tombolo formation are similar to those observed in the growth of spits, bars and barrier islands (Anthony and Blivi, 1999; Blivi et al., 2002). Tombolos develop in shallow areas behind island barriers, where sufficient sediment supply coupled with wave and wind action are favourable to beach accretion. Tides, swell and currents serve as the transporting media, interacting with the island to set up a complex pattern of wave refraction and diffraction on the lee of the obstacle.

In terms of sequence stratigraphy tombolos are part of the Highstand Systems Tract (Catuneanu, 2002, 2005; Cattaneo and Steel, 2003) and, like deltas and estuaries, the inception of their prograding sediment wedges is dated to approximately 8000 to

* Corresponding author.
E-mail address: nick.marriner@wanadoo.fr (N. Marriner).

0169-555X/$ - see front matter © 2008 Elsevier B.V. All rights reserved.
doi:10.1016/j.geomorph.2008.01.013

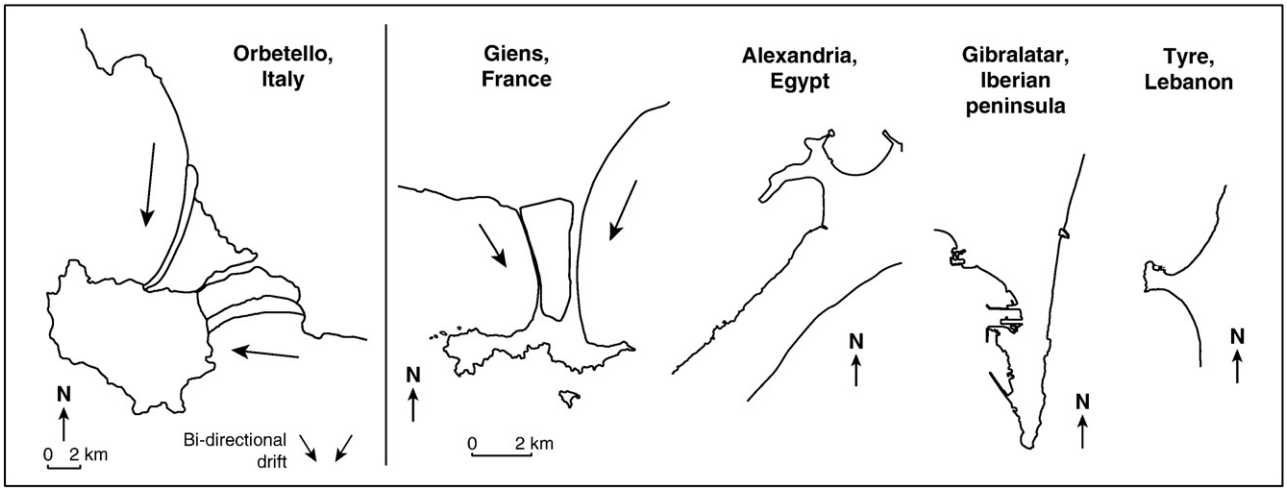

Fig. 1. Tyre's tombolo set against some of the Mediterranean's better known examples.

6000 BP (Stanley and Warne, 1994). They comprise triangular forms, widest at the base – where the initial accretion begins – thinning laterally towards the island obstacle. The scales of these landforms can vary considerably from just a few tens of metres behind small obstacles up to 15 km as in the case of Orbetello on the Italian coast (Fig. 1; Gosseaume, 1973). Although single tombolo bridges tend to be the rule, there are good examples of tombolo pairs (for example Giens, France, see Blanc, 1959; Courtaud, 2000) and even triplets (Orbetello, Italy, see Gosseaume, 1973) from the Mediterranean. Double tombolo formation is attributed to waves approaching the island flanks at different angles of incidence, with lagoons developing in the sheltered area between the twin salients (Blanc, 1959).

The overriding requirements for tombolo formation are: (1) high sediment supply, for example at the margin of river mouths; (2) a physical barrier against the swell; and (3) coastal processes conducive to the development of a sand bank, i.e., bi-directional currents converging towards this physical barrier (Davies, 1980).

Here, we report stratigraphic and geomorphological data from the isthmus of Tyre in Lebanon. Juxtaposed against other circum-Mediterranean examples (e.g. Orbetello, Giens, Gibraltar and Alexandria), Tyre is a small sedimentary system rendering it ideal for scientific inquiry and the formulation of a stratigraphic model (Fig. 2). These data are then compared and contrasted with research undertaken on Alexandria's tombolo at the margin of the Nile delta in Egypt (Goiran, 2001; Goiran et al., 2005).

2. Meteo-marine and geomorphological contexts

The coastal plain in the Tyre vicinity reaches a width of 2–3 km. This is atypical of the south Lebanese coastline which is otherwise dominated by a series of Cenomanian and Eocene headlands that protrude into the sea (Dubertret, 1955; Sanlaville, 1977). Tyre lies upon an uplifted horst, bounded to the east by the Roum fault and to the south by the Rosh Hanikra–Ras Nakoura fault (Morhange et al., 2006). A series of ENE-trending faults intersect the Tyrian coastal plain putting into contact the Cenomanian and Eocene geology. The coastal plain is dominated by both consolidated and clastic Quaternary deposits. Throughout the Holocene, the Tyrian coastline has been protected by a broken chain of sandstone outcrops, part of a drowned N–S ridge that runs parallel to the coastline (Dubertret, 1955; Sanlaville, 1977). The oblique stratification of the latter indicates that they are aeolian in origin. The sandstone ridges are locally referred to as 'ramleh' and are the chronostratigraphic analogues of the 'kurkar' ridges rimming the Israeli coast (Frechen et al., 2001, 2002, 2004; Sivan and Porat, 2004). These Quaternary outcrops have dampened the effects of the swell, and aerial photographs show an intricate pattern of wave diffraction in the lee of Tyre island. The defensive location and natural anchorages afforded by these offshore sandstone ridges attracted human societies from the Bronze Age onwards (Marriner et al., 2006). Successive cultures, including Canaan, Phoenician, Persian, Hellenistic, Roman and Byzantine have significantly marked and modified the coastal landscapes (Katzenstein, 1997; Doumet-Serhal, 2004; Marriner, 2007; Marriner et al., in press).

Despite early attempts by Nabuchodonozor II to link Tyre to the mainland during the 6th century BC (Fleming, 1915; Nir, 1996; Katzenstein, 1997), stratigraphic data demonstrate that the city remained an island until 332 BC, separated from the continent by ~800–1000 m of sea (Marriner et al., 2007). Following stubborn resistance by the Tyrians, Alexander the Great cleverly exploited the shallow bathymetry induced by Tyre's proto-tombolo, to build a causeway and breach the island's insularity. When the city eventually fell to the Macedonian armies, the causeway was strengthened using rubble from destroyed quarters of the city (see Diodorus Siculus, writing in the 1st century BC, 1967). In its most advanced stage, it is speculated that the sea-bridge reached an average width of 200 Greek feet, or ~60 m (Nir, 1996). This engineering feat, a prototype for Alexandria's causeway built a year later, significantly artificialised the coastline and accelerated accretion of the salient.

Tyre's tombolo comprises a W–E-trending salient, 1500 m long by 3000 m wide (Fig. 2), and lies ~9 km south of the Litani embouchure. The Litani is Lebanon's most important fluvial system, transiting $\sim 284 \times 10^6$ m^3 of sediment per year (Abd-el-Al, 1948; Soffer, 1994). Previously performed clay mineralogical

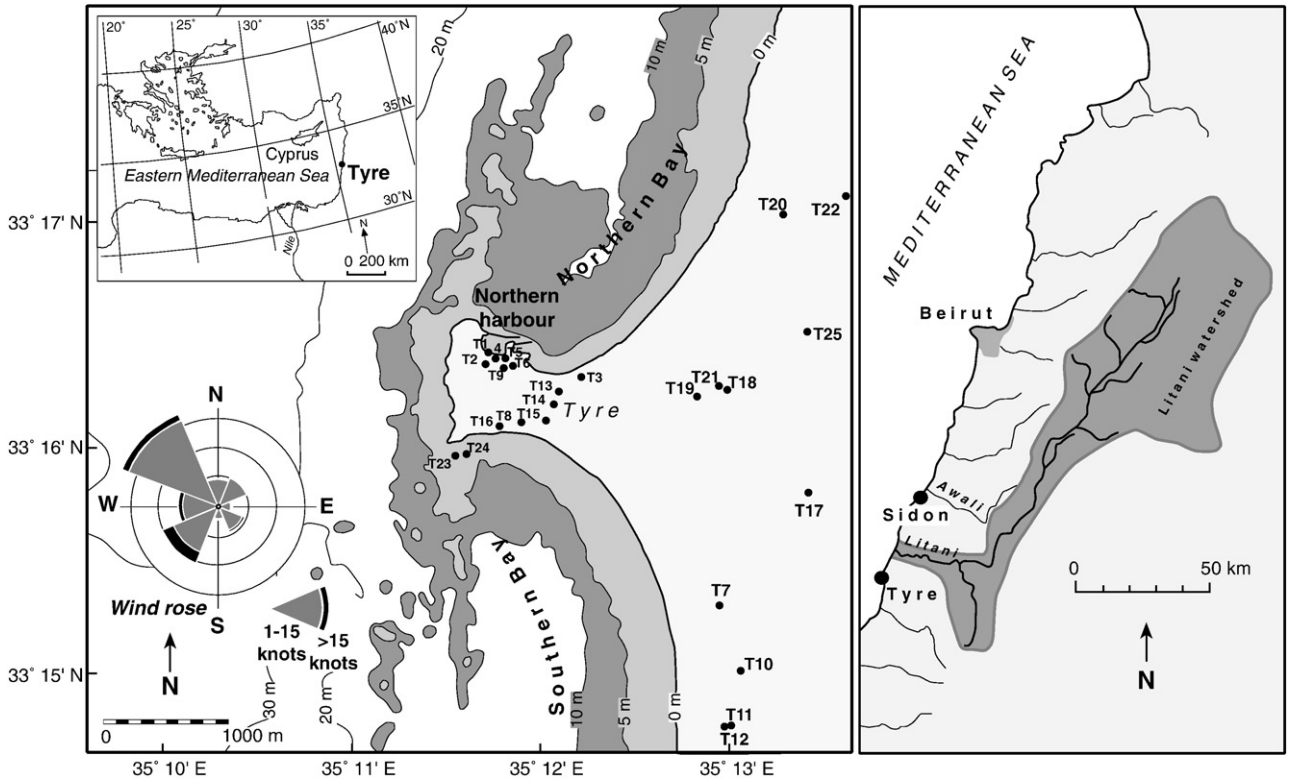

Fig. 2. Location of core sites on the Tyrian peninsula (black dots denote the sites).

analyses indicate that it has been one of the primary sediment sources for the isthmus during the Holocene (Marriner, 2007). The Litani yields a unique clay composition comprising illite–smectite phases (50–60%) and kaolinite (40–50%). Very high kaolinite content is unique to south Lebanon, with all fluvial systems between the rivers Litani and Awali manifesting similar mineralogical signatures (Ribes et al., 2003).

The Tyrian coastline is subject to a microtidal wave regime (<45 cm). In light of this, wave impact, longshore currents and swell diffraction are the key factors driving tombolo formation. Dominant coastal winds and swell derive from the south-west, with periodic north-westerlies giving rise to bi-directional drift. Wave climatological data attest to high-energy sea-states; wave heights of more than 5 m are measured every ~2 years, and greater than 7 m every ~15 years (Rosen and Kit, 1981; Goldsmith and Sofer, 1983; Carmel et al., 1985a,b). The site is exposed to a wide swell window with a fetch of ~750 km from the northwest and ~650 km from the southeast.

3. Methods and data acquisition

3.1. Field data acquisition

At Tyre, a total of 25 cores was obtained (Fig. 2). Sediments were extracted using a 10 cm by 200 cm mechanised corer. Core sections were lined with a protective sleeve to avoid sediment slumping. All cores were GPS levelled and depths quoted on logs have been benchmarked against mean biological sea level (i.e. the maximum height of the subtidal zone, Laborel and Laborel-Deguen, 1994). This benchmark was established using the upper limit of living *Balanus* populations growing on the modern harbour quay faces. At Alexandria, 13 cores were drilled along the city's present seaboard (Fig. 3). Here we present stratigraphic data from two cores, C2 and C9, deriving from the tombolo, either side of Alexander the Great's Heptastadium (Hesse, 1998). Following extraction, all cores were stored in cold rooms at the CEREGE geoscience facilities in Aix-en-Provence, France.

3.2. Sediment analysis

Initial facies descriptions (e.g. colour, petrofacies) were undertaken under standardised laboratory conditions, before sampling to establish general stratigraphy. Samples were oven dried at 40 °C and subsequently described using the Munsell colour scheme. Dry sediment aggregates were weighed and washed through two mesh sizes, 2 mm and 50 μm, to separate out the gravel (>2 mm), sand (2 mm to 50 μm) and silt and clay (<50 μm) fractions. In most cases, 100 g of dry aggregate were washed through to ensure the statistical validity of the results. The dried fractions were weighed and data plotted against stratigraphic logs in percentages.

The sand fraction was subjected to mechanical sieving. At least 50 g of dry sands were used. These were mechanically sieved using 15 meshes descending in size from 1.6 mm to 0.063 mm, and accordingly weighed. Statistical analyses were subsequently performed to establish various grain size parameters such as histograms, fractiles and graphical indices.

Fig. 3. Location map of core sites at Alexandria.

3.3. Biostratigraphy

Identification of molluscan shells was undertaken upon the retained gravel fraction and assigned to assemblages according to the Péres and Picard (1964), Péres (1982), Barash and Danin (1992), Poppe and Goto (1991, 1993), Bellan-Santini et al. (1994), Bitar and Kouli-Bitar (1998) and Doneddu and Trainito (2005) classification systems. Both *in situ* and *extra situ* taxa were identified.

Ostracoda were extracted from the dry sand fraction (>150 μm). A minimum of 100 valves was identified and assigned to five assemblages on the basis of their ecological preferences: fresh water, brackish lagoonal, marine lagoonal, coastal and marine.

3.4. Chronostratigraphy

Radiocarbon dates and numerous archaeological data precisely constrain the chronology of the various sedimentary environments observed (Table 1). All dates have been calibrated using OxCal version 3.10, and are quoted to 2σ (Bronk Ramsey, 2001). Material dated included seeds, wood and charcoal remains, and *in situ* molluscan marine shells (corrected for reservoir effects during calibration).

3.5. Numerical models

At Tyre the stratigraphic datasets are based upon a series of four cores (see Fig. 2), 8 to 16 m in depth. A N–S transect was obtained with an aim to elucidate the stages of accretion of the sedimentary bodies. With the collaboration of S. Meulé (CEREGE CNRS), a swell propagation model was run for bathymetries at 5500 BP and 2000 AD, to better understand the diffraction of the swell by the breakwater island (Marriner et al., 2007). Bathymetric data were derived from the 1998 SHOM marine map of the Tyrian coastal area (Service Hydrographique et Océanographique de la Marine, 1998, Ports du Liban, 7514, 1:25000) and coupled with our chronostratigraphic datasets to obtain a representative coastal reconstruction of Tyre at ~5500 BP. Based on our observations of the archaeology and coastal stratigraphy, a local 5 m relative sea-level rise was factored into this reconstruction. The model used equations from the Steady-State Spectral Wave Model (STWAVE) with a JONSWAP swell spectrum (McKee Smith et al., 2001). A total of six model runs was completed for swell scenarios at 2000 AD from 225°, 270° and 315°, and at 5500 BP at 225°, 270° and 315° (dominant swell direction). Wave spectra were generated for each angle scenario using a standard swell height of 2.6 m with a period of 6 s. Each spectrum was subsequently propagated over the

Table 1
Radiocarbon dates for Tyre (no shading) and Alexandria (shading)

Sample	Code	Sample	$^{13}C/^{12}C$ (‰)	^{14}C BP	±	Cal. BP	Cal. BC/AD
T13-9	Poz-9943	1 *Tricolia pullus*	0.9	2650	35	2470–2230	520 BC–280 BC
T13-15	Poz-9898	4 *Rissoa* sp.	2	2870	30	2730–2510	780 BC–560 BC
T13-21	Poz-9944	6 *Rissoa* sp.	−1.9	2980	35	2840–2690	890 BC–740 BC
T13-25	Poz-9945	2 *L. lacteus*	4.7	7450	40	8000–7820	6050 BC–5870 BC
T13-39	Poz-13916	1 *Parvicardium exiguum*		7210	40	7780–7580	5830 BC–5630 BC
T14-6	Poz-13964	*Donax semistriatus*	−0.3	2245	30	1950–1750	0 AD–200 AD
T14-14	Poz-12137	1 *Tricolia pullus*	3.3	2795	30	2680–2400	730 BC–450 BC
T14-20	Poz-13915	3 *Bittium* spp., 1 *Rissoa* sp., 1 *Venus casina*	−0.4	6370	35	6950–6730	5000 BC–4780 BC
T14-23	Poz-12136	4 *L. lacteus*	3.3	7840	40	8390–8190	6440 BC–6240 BC
T15-19	Poz-12154	1 *Nassarius reticulatus*	−0.4	2385	30	2120–1910	170 BC–40 AD
T15-25	Poz-13965	2 *Mitra ebenus*	4	5775	35	6280–6100	4330 BC–4150 BC
T15-26	Poz-12133	3 *L. lacteus*	4.4	5740	35	6270–6020	4320 BC–4070 BC
T15-30	Poz-12134	1 *Cerithium vulgatum*, 2 *P. exiguum*	4.3	7680	40	8270–8020	6320 BC–6070 BC
T18-39	Poz-13966	1 *Parvicardium exiguum*	−5.6	4180	30	4380–4150	2430 BC–2200 BC
T18-59	Poz-9946	1 *Neverita josephinae*	−0.8	5710	40	6240–5990	4290 BC–4040 BC
T18-64	Poz-9900	1 *L. lacteus*	3.7	5980	40	6490–6290	4540 BC–4340 BC
C2-7	Ly-1521	Shells	0	1530	35	1180–970	770–980 AD
C2-8	Ly-1522	Shells	1.05	1635	35	1280–1100	670–850 AD
C2-9	Ly-8873	Clays	–	1720	45	1360–1170	590–780 AD
C2-14	Ly-1305 (OxA)	AMS	0.21	1845	45	1510–1290	440–660 AD
C2-15	Ly-10567	Shells	1.28	1935	55	1630–1340	320–610 AD
C2-18	Ly-8871	*Cladocora*	−2	4195	50	4420–4120	2470–2170 BC
C2-20	Ly-10570	*Cladocora*	−2.74	4640	50	5030–4770	3080–2820 BC
C2-25	Ly-8870	*Cladocora*	−2.6	5360	55	5870–5600	3920–3650 BC
C2-27	Ly-8869	Shells	1.3	7810	55	8390–8160	6440–6210 BC
C9-20	Ly-10615	*Cladocora*	−2.24	2330	40	2070–1830	120 BC–120 AD
C9-28	Ly-10617	*Cladocora*	−2.26	5485	50	5980–5720	4030–3770 BC

digitised bathymetry to yield data outputs on swell compass direction (Dir), significant wave height of swell (Hs) and the peak period of the swell in seconds (Tp). Numerical output files comprised a grid area 99 cells N–S by 65 cells E–W, yielding a total of 6425 data points.

4. Results

4.1. Chronostratigraphic results

Here we describe the stratigraphic data obtained from four Tyrian cores.

4.1.1. Core T18 El Bass/Mashuk salient base: description

Core T18 was drilled between Tell Mashuk and El Bass. This area comprises the oldest part of the subaerial salient *sensu stricto*; the sedimentary record attests to the accretion and progradation of the beach ridges from 6000 BP onwards. The clay substratum is transgressed by a fine-bedded marine sand (unit A) dated to ~6000 BP (Figs. 4–5). Unit A is dominated by molluscs from the subtidal sands (*Bittium* sp., *Tricolia pullus*, *Rissoa lineolata*) and silty or muddy-sand assemblages (*Nassarius pygmaeus*, *Macoma* sp., *Macoma cumana*, *Rissoa monodonta*). Marine-lagoonal (*Loxoconcha* spp., *Xestoleberis* sp.) and coastal (*Aurila convexa*, *Pontocythere* sp., *Urocythereis* sp.) ostracod taxa characterise the unit. The unit records rapid beach ridge accretion and by ~5500 BP, a protected environment is indicated by the litho- and biostratigraphic proxies (units B and C).

In unit B, diagnostic beach sedimentology at the base shallows up to a lagoon environment. The top of the facies is dated to 4180±30 ^{14}C years BP, or 2430–2200 cal. BC. The sparse molluscan indicators are exclusively dominated by *Cerastoderma glaucum*, a lagoon-tolerant taxa. In unit C, the silts and clays comprise >95% of the total sediment fraction. This fine-grained sedimentology, allied with sparse tests of *C. glaucum*, concurs continued lagoonal conditions. We hypothesise the existence of a shallowing-up sediment-choked lagoon, which could have served as an anchorage haven during the Bronze Age (Marriner et al., in press). Unit D constitutes a brown clay lithofacies dated to Roman times. The unit did not yield any marine fauna; plant macrorests and fossil snail tests are concurrent with a marsh environment that persisted in the El Bass area until 1864, after which time it was drained for agricultural and sanitary purposes (Carmona and Ruiz, 2004).

4.1.2. Core T13: description

Core T13 derives from the septentrional lobe of the tombolo, just north of the ancient causeway. Around 10 m of Holocene fill records the marine transgression and progradation of the northern flank of the tombolo. The transgression is dated to ~8000 BP and is onlapped by a poorly sorted shelly silt and fine sand unit (Fig. 6). Unit A is lithodependent, with reworking of the underlying clay substratum (Cohen-Seffer et al., 2005). The ostracod fauna is dominated by the brackish-lagoonal species *Cyprideis torosa*, with minor peaks of marine-lagoonal (*Loxoconcha* spp.) and coastal (*A. convexa*, *Aurila woodwardii*) taxa (Fig. 7). A

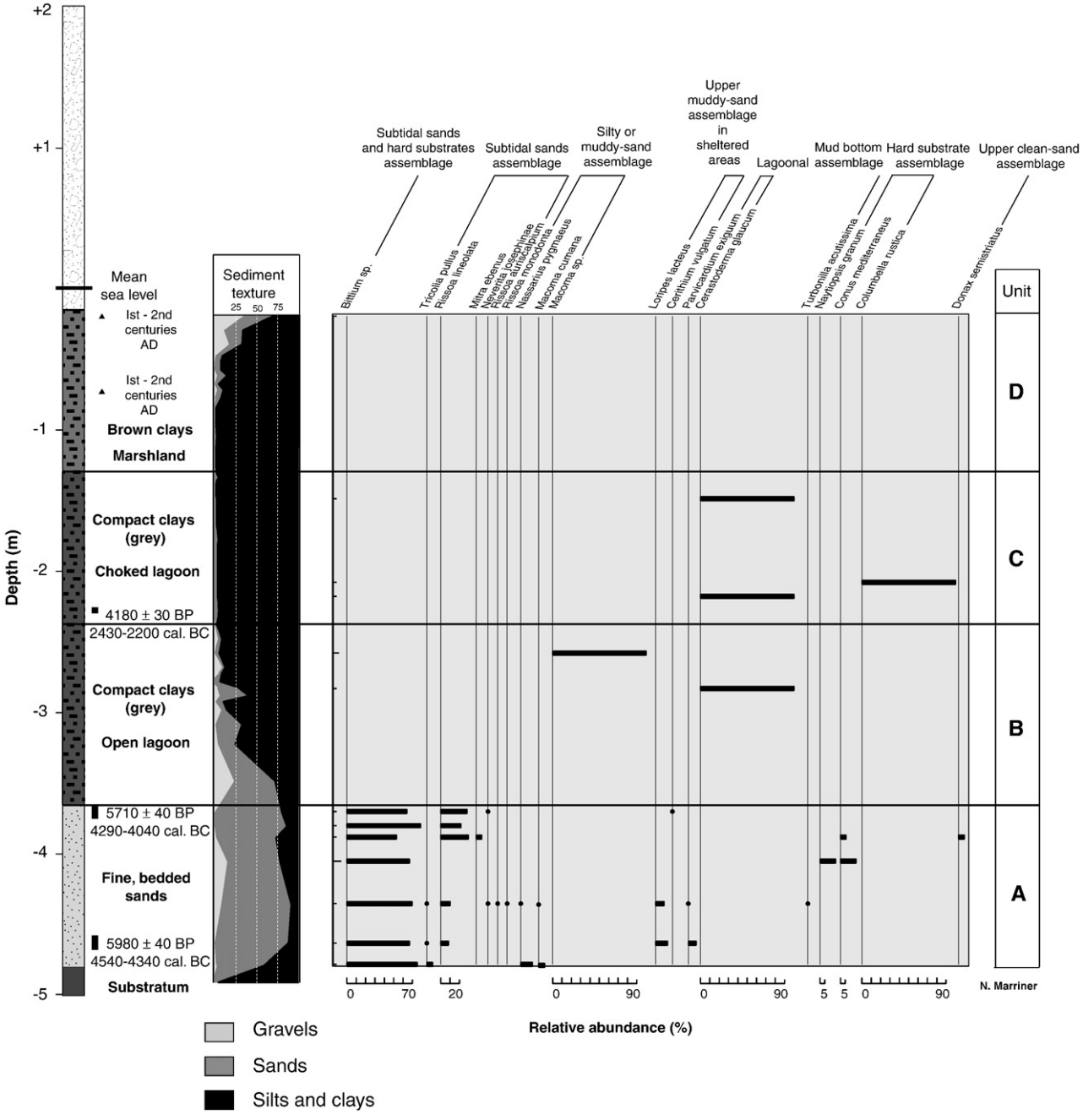

Fig. 4. Core T18 marine macrofauna.

protected marginal marine environment is corroborated by the macrofauna suites comprising taxa from the upper muddy-sand assemblage in sheltered areas (*Cerithium vulgatum*, *Loripes lacteus*), subtidal sands assemblage (*R. lineolata*, *Rissoa scurra*, *Mitra ebenus*) and the lagoonal assemblage (*Parvicardium exiguum*, *Hydrobia acuta*, *C. glaucum*, Fig. 8).

After ~7000 BP, transgressive ridges eventually breached the area, with an onshore movement of coarse sand and gravel (unit B). The unit is characterised by the following macrofauna assemblages: subtidal sands, upper muddy-sand assemblage in sheltered areas and the hard substrate assemblage. A sharp decline in *C. torosa* is countered by peaks of marine-lagoonal and coastal ostracod species. Outer marine species such as *Semicytherura* spp., *Callistocythere* spp. and *Neocytherideis* sp. were also drifted in.

Around 3000 BP, against a backdrop of decelerating sea-level rise (Sivan et al., 2001), we record the rapid accretion of a well-sorted fine sand lithofacies (unit C). The subtidal sand and hard substrate taxa *Bittium reticulatum* and *Turboella similis* dominate the unit. High relative abundances of marine-lagoonal and coastal ostracod taxa are consistent with a middle to low-energy shoreface. The top of unit D is dated 2650±35 ^{14}C BP. Factoring in ~3 m of RSL change since antiquity, this suggests a proto-tombolo surface within 2±1 m of the water surface by

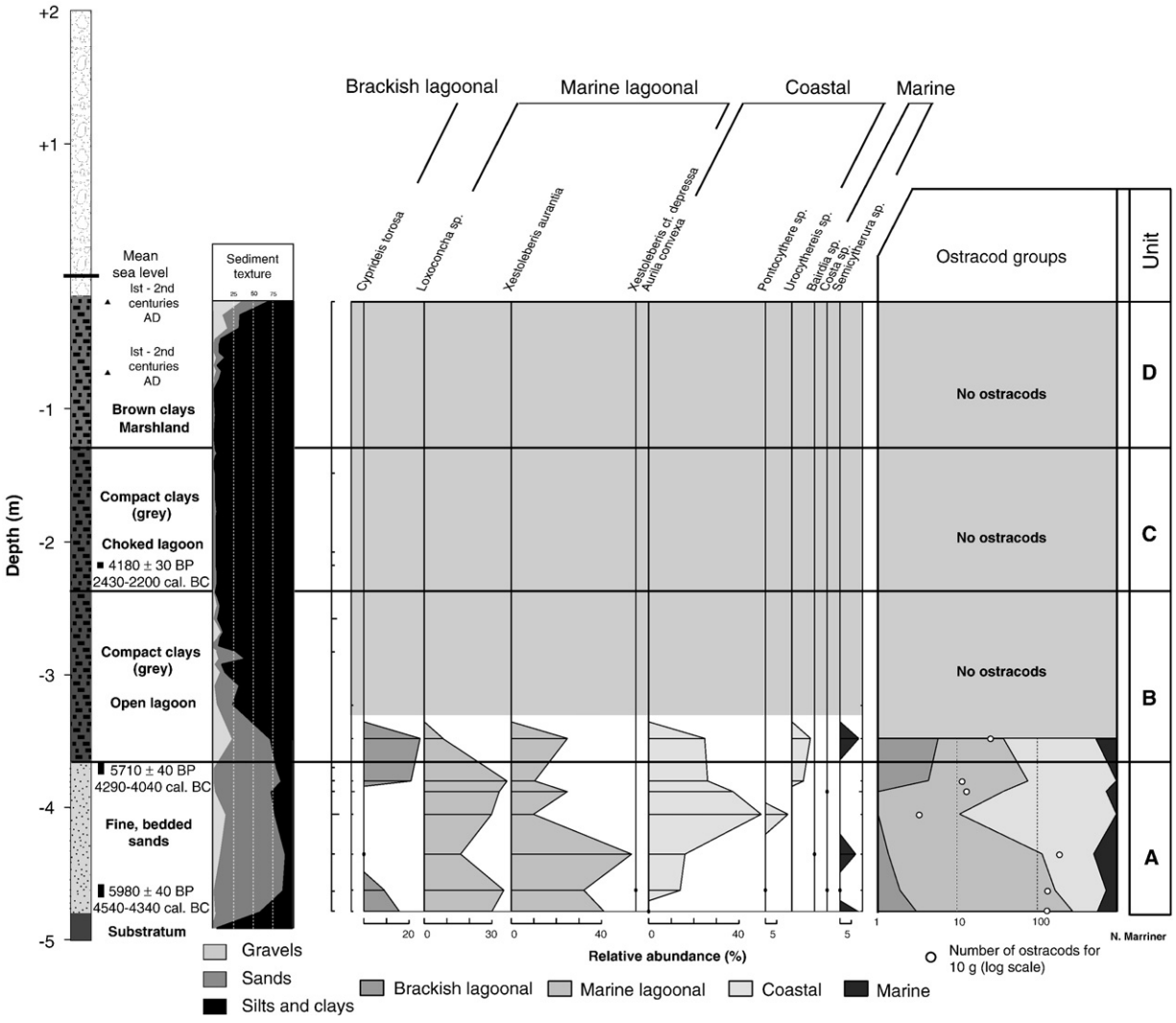

Fig. 5. Core T18 ostracods.

the 4th century BC. Unit E comprises a poorly sorted, coarsening-upward sediment devoid of macro- and microfossils. We ascribe this to a prograding Byzantine shoreface.

4.1.3. Core T14: description

Core T14 lies 120 m south of core site T13, on the opposite side of the causeway. The marine flooding surface is dated to ~7800 BP by a poorly sorted sand unit which transgresses the clay substratum (Fig. 9). Fine sand and a shelly gravel fraction characterise the sediment texture. Four ecological groups dominate the unit's macrofauna suite: the upper clean-sand assemblage (*Pirenella conica*), the subtidal sand assemblage (*R. lineolata*, *Rissoa dolium*, *M. ebenus*), the upper muddy-sand assemblage in sheltered areas (*L. lacteus*, *C. vulgatum*), lagoonal (*P. exiguum*, *Hydrobia ventrosa*) and the subtidal sands and hard substrates assemblage (*B. reticulatum*). The ostracod fauna is dominated by the brackish-lagoonal species *C. torosa*, with the presence of marine-lagoonal taxa such as *Loxoconcha* spp. and *Xestoleberis aurantia* (Fig. 10). These litho- and biostratigraphic indicators translate to a low-energy lagoonal environment, protected from the open sea by beach and berm transgressive ridges (Otvos, 2000). Small peaks of coastal and marine taxa are concurrent with phases of breaching of these protective barriers during storm episodes.

Unit B comprises an aggrading silty-sand unit. Molluscan tests are absent from the unit and the ostracod faunal density is low, with just a few tests of the coastal species *A. convexa*. It is overlain by unit C, a poorly sorted gravely sand unit characterised by weakly developed grain size histograms, typical of a beach shoreface. Poorly preserved hard substrate molluscan tests (*Gibbula varia*, *Fusinus pulchellus*, *Chama gryphoides*, *Cantharus pictus*, *Conus mediterraneus*) and the absence of an ostracod fauna concur high-energy swash zone dynamics characterised by the reworking of imported molluscan tests. The chronology is coeval with a Hellenistic beach face (2795±30 ^{14}C BP, T14-14).

Unit D is characterised by a well-sorted silty-sand unit. The molluscan fauna is poor, with rare tests of *in situ Donax semistriatus* (upper clean-sand assemblage) indicating rapid rates of sedimentation that hinder the development of a biocenosis. The ostracod faunas are dominated by the marine-lagoonal species *Loxoconcha* spp. and *X. aurantia*, with smaller

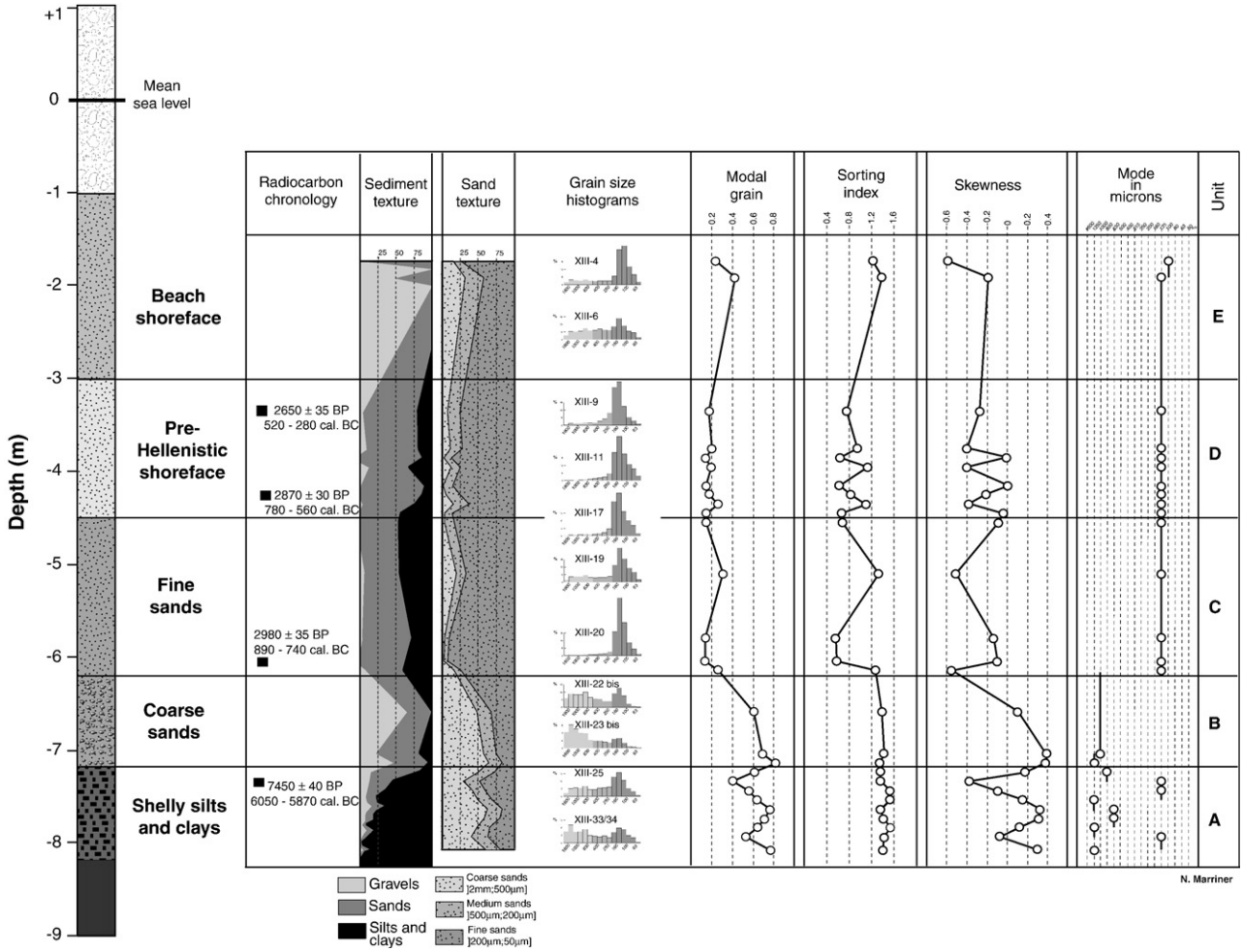

Fig. 6. Core T13 lithostratigraphy and grain size analyses.

peaks of coastal taxa such as *A. convexa* and *Aurila* sp. The top of the unit is dated 2245±30 ^{14}C BP (0–200 cal. AD) and attests to rapid rates of salient accretion following the construction of Alexander's causeway. This rapid salient growth significantly hindered longshore drift. A fall in water competence around the causeway is indicated by the fine-grained nature of the unit and high relative abundances of marine-lagoonal taxa.

4.1.4. Core T15: description

Core T15 lies 250 m to the south of the ancient causeway. 16.5 m of fill have accumulated since 8000 BP. As with the other tombolo cores, the basal unit A comprises a silty-sand unit with large amounts of shell debris (Fig. 11). Upper muddy-sand assemblage in sheltered areas and subtidal sands macrofauna assemblages dominate. Brackish-lagoonal (*C. torosa*) and marine-lagoonal (*Loxoconcha* spp., *X. aurantia*) ostracod taxa characterise the microfossil fauna, data which corroborate the existence of a sheltered lagoon environment (Fig. 12). In unit B, transition to a poorly sorted coarse sand fraction is consistent with retrograding berm ridges, reworking sediment stocks as the forms transgressively onlap the lagoon environment. A rise in marine-lagoonal (*Loxoconcha* spp., *X. aurantia*) and coastal ostracod taxa (*A. convexa*, *A. woodwardii*) is to the detriment of the formerly abundant *C. torosa*.

Unit C constitutes a well-sorted, fine grey sand unit concomitant with those observed in cores T13 and T14. The unit is characterised by marine-lagoonal ostracod taxa, with small peaks of coastal species (*A. convexa*, *Urocythereis oblonga*, *Neocytherideis* sp.). The base of the unit is void of an ostracod fauna.

Unit D comprises a coarser beige sand, analogous with a coarsening-up sequence. A rise in coastal ostracod taxa is coeval with an accreting subaqueous salient. Marine species such as *Semicytherura* sp., *Costa* sp., *Callistocythere* spp., *Basslerites berchoni* and *Bairdia* spp. were drifted in during periods of heightened swell and storms. Fine-grained sedimentary conditions persist into unit E, which is dominated by marine-lagoonal and coastal ostracod taxa.

4.2. Swell propagation model

For simulations of the coast at 5500 BP, the effects of swell diffraction and shoaling are clearly manifested. The incoming swell, which is initially quasi-unidirectional (225°, 270° or 315°), is spread by the lateral movement of energy into the shadowed area behind Tyre island. Projections at 5500 BP indicate that the

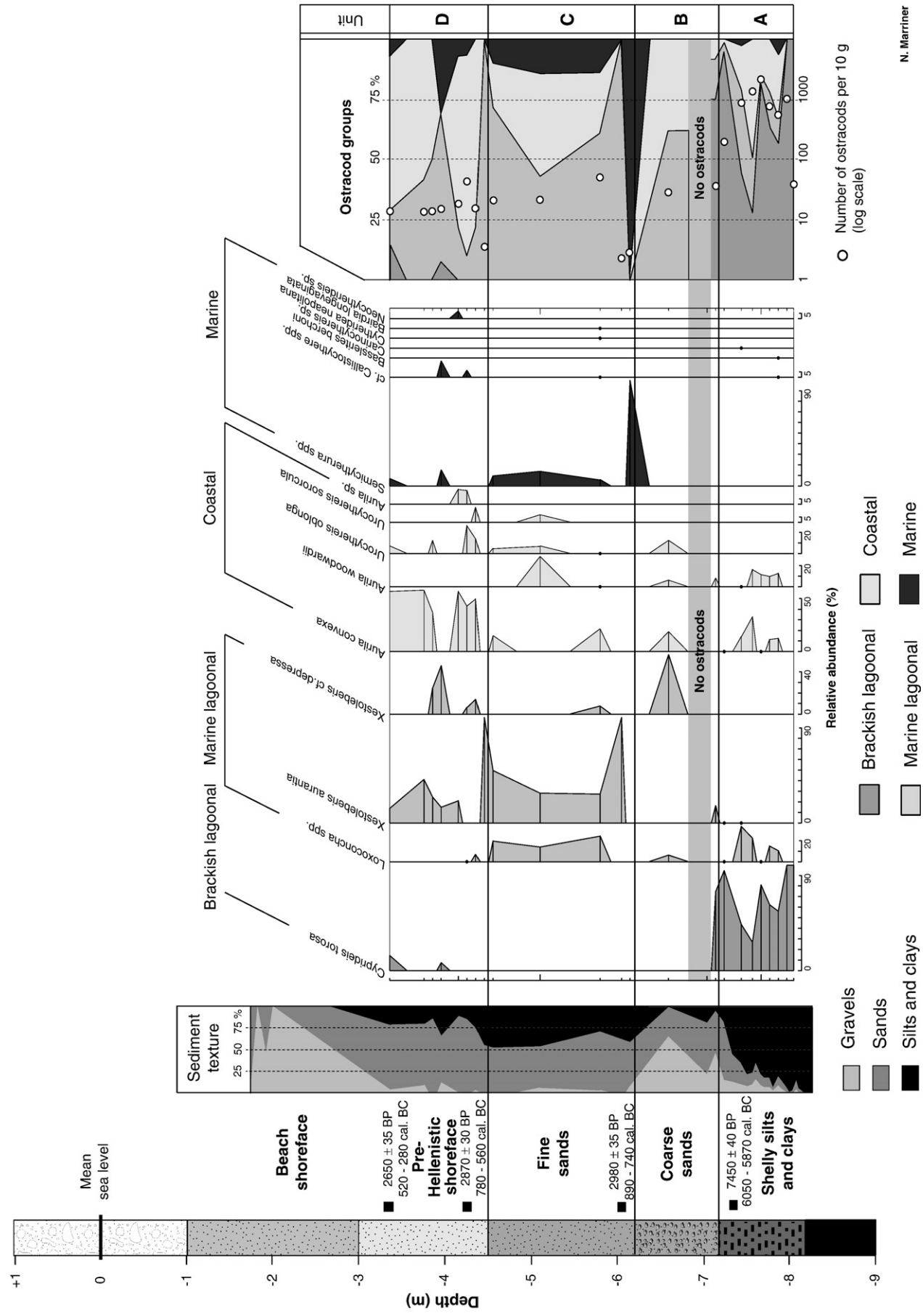

Fig. 7. Core T13 ostracods.

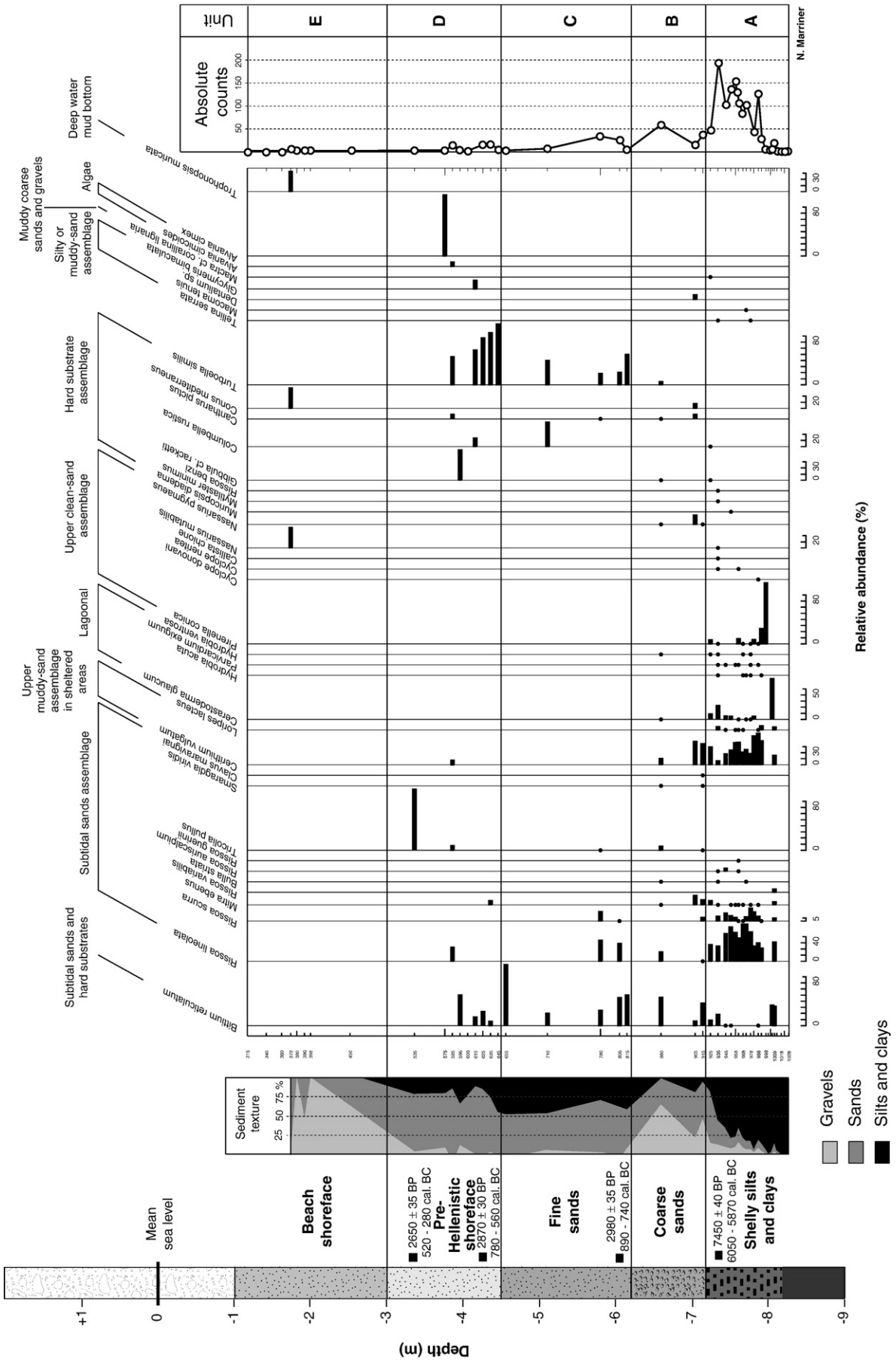

Fig. 8. Core T13 macrofauna.

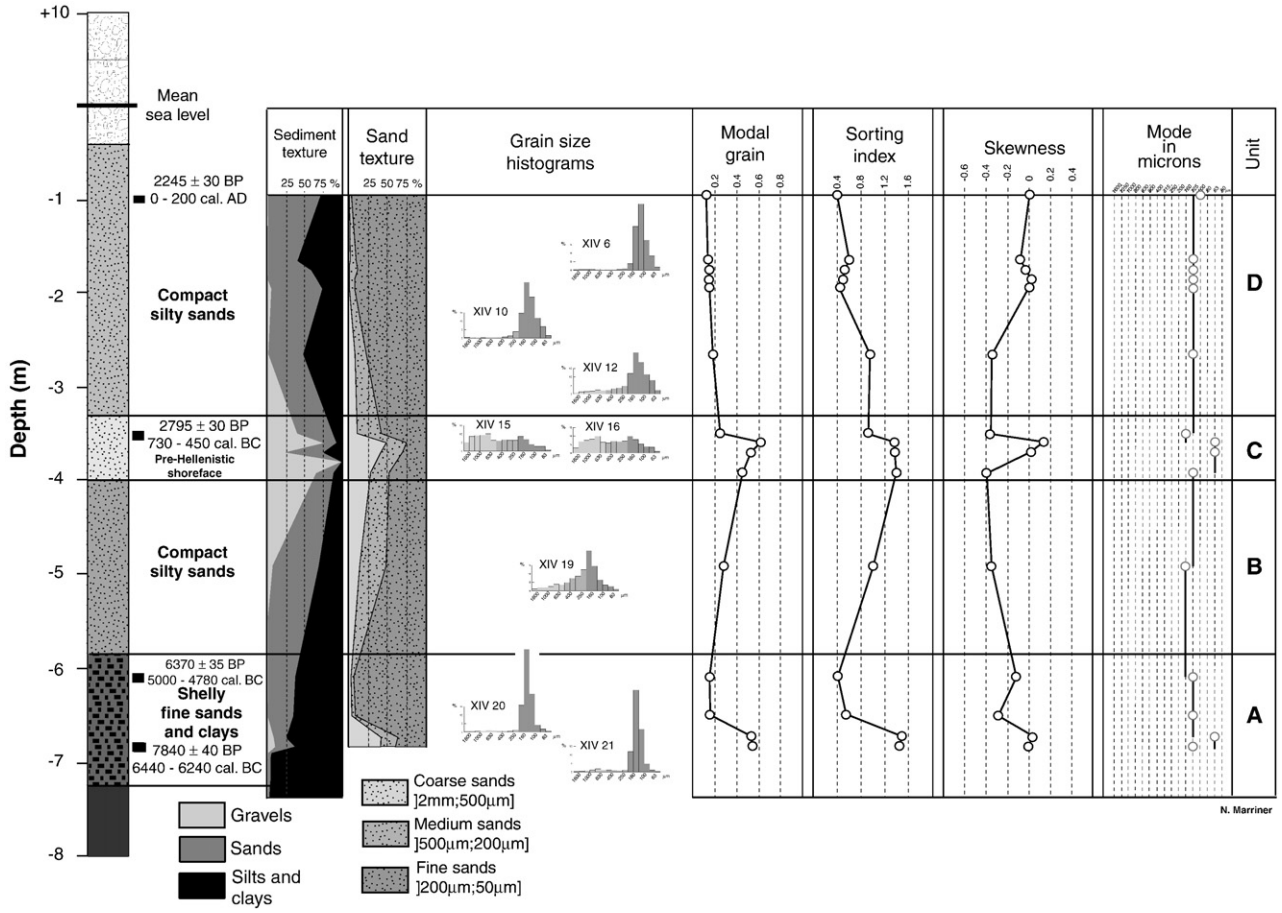

Fig. 9. Core T14 lithostratigraphy and grain size analyses.

majority of the swell incident energy is blocked by the natural N–S-trending breakwater (Fig. 13). As the wave energy that passes the obstacle spreads laterally into the shadow region, the total energy is distributed over a broader area reducing the swell height leeward of the island from >1.80 m west of the island to <0.75 m on the eastern shadow side (propagated wave height is 2.6 m with a period of 6 s). This shadow generated a significant natural shelter zone for the offshore anchoring of boats, greatly increasing the anchorage capacity of the city (Marriner et al., 2007). The core transect falls in an area of very low wave height (~0.40 m), evoking the rapid accretion of the marine bottom. We conclude that the early accretion of the proto-tombolo took place in two areas: (1) *along the continental margin of Tell Mashuk* the sedimentological data show that limited accommodation space led to the rapid progradation of a salient strandplain, as corroborated by low wave heights along the coastal fringe; (2) *secondarily in the wave shadow behind Tyre island* the models show a sharp fall in energy accompanied by a concomitant marine bottom shallowing. The greater accommodation space means, however, that the tombolo remained a subaqueous form in this zone. By a process of positive feedback, the shallowing bathymetry altered the pattern of diffraction and refraction leading to the shallowing of deeper distal areas between the island and the continent. A bi-directional drift pattern was also created by the island obstacle.

Late Roman tectonic subsidence (Morhange et al., 2006) means that the breakwater effects of Tyre island are much less pronounced today than for 5500 BP. A significant wave shadow is generated to the north and south of the tombolo for projections at 225° and 315°. Meteorological data indicate that although the strongest winds and swell derive from the south-west, north-westerlies are also very frequent (33% of total winds). North-westerly swell diffraction and refraction appear to be the main transport mechanisms in translating Litani sediments to the Tyrian peninsula. The models suggest that westerly winds and swell, though less frequent than the dominant south-westerlies and north-westerlies, were also significant in forcing the initial accretion of the sand bank.

5. Discussion and interpretations

Here we marry the chronostratigraphic and modelling data to report details on the Holocene morphodynamics and process-response of Tyre's tombolo. We then compare this three-phase model with Alexandria's tombolo.

5.1. Three-phase model of tombolo morphogenesis

High-resolution analyses shed light on three important geomorphological aspects: (1) natural accretion of Tyre's early

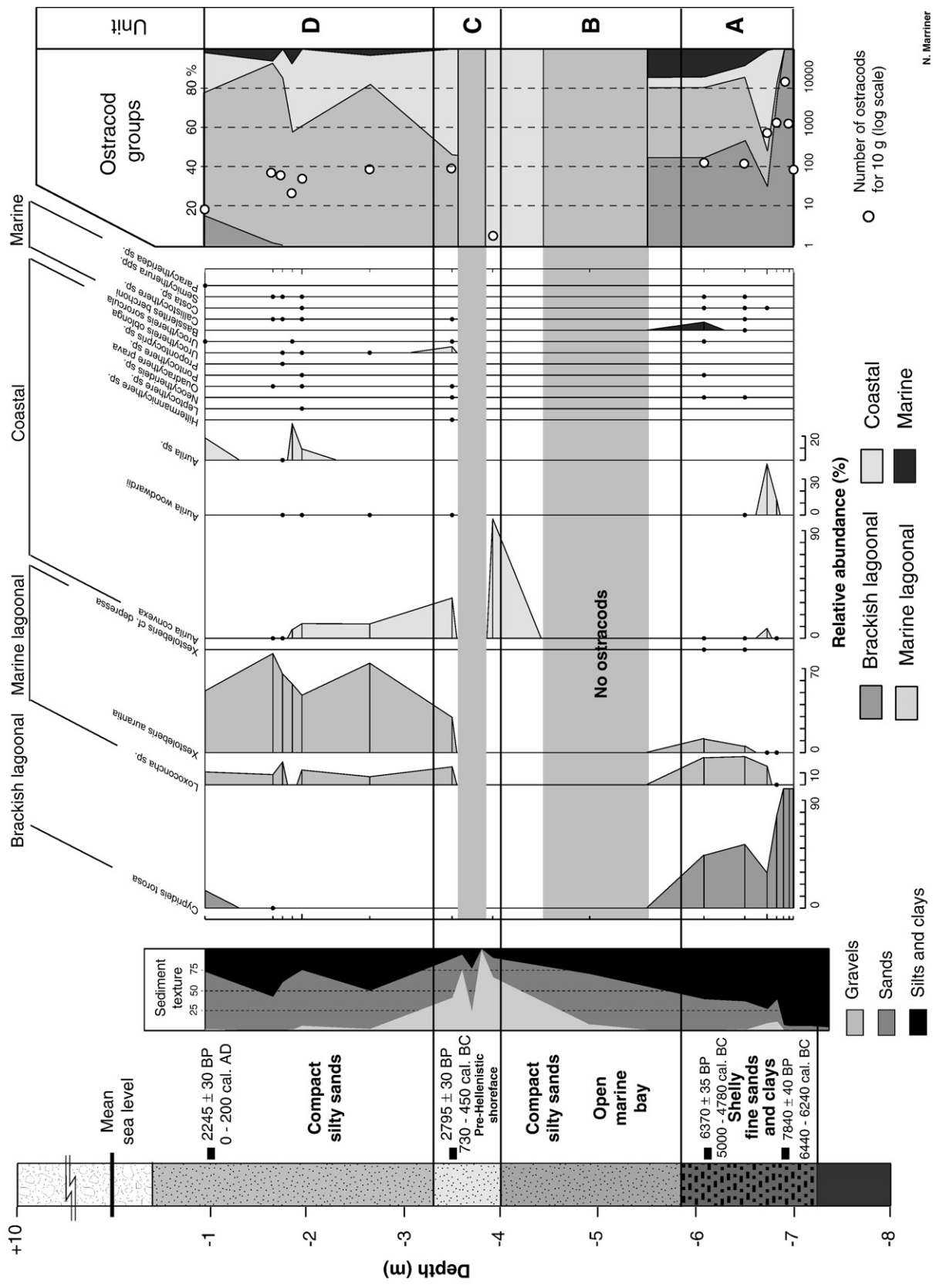

Fig. 10. Core T14 ostracods.

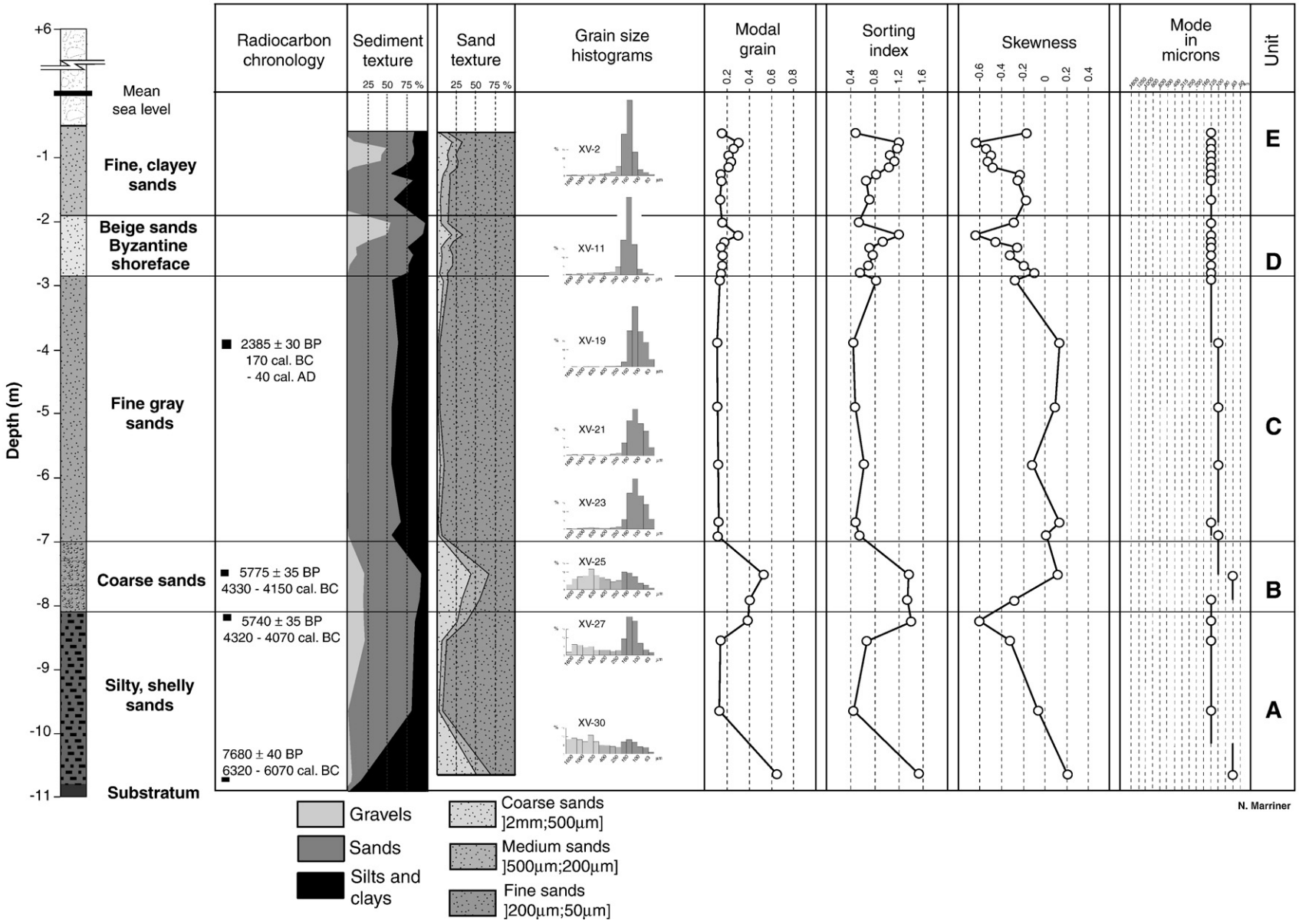

Fig. 11. Core T15 lithostratigraphy and grain size analyses.

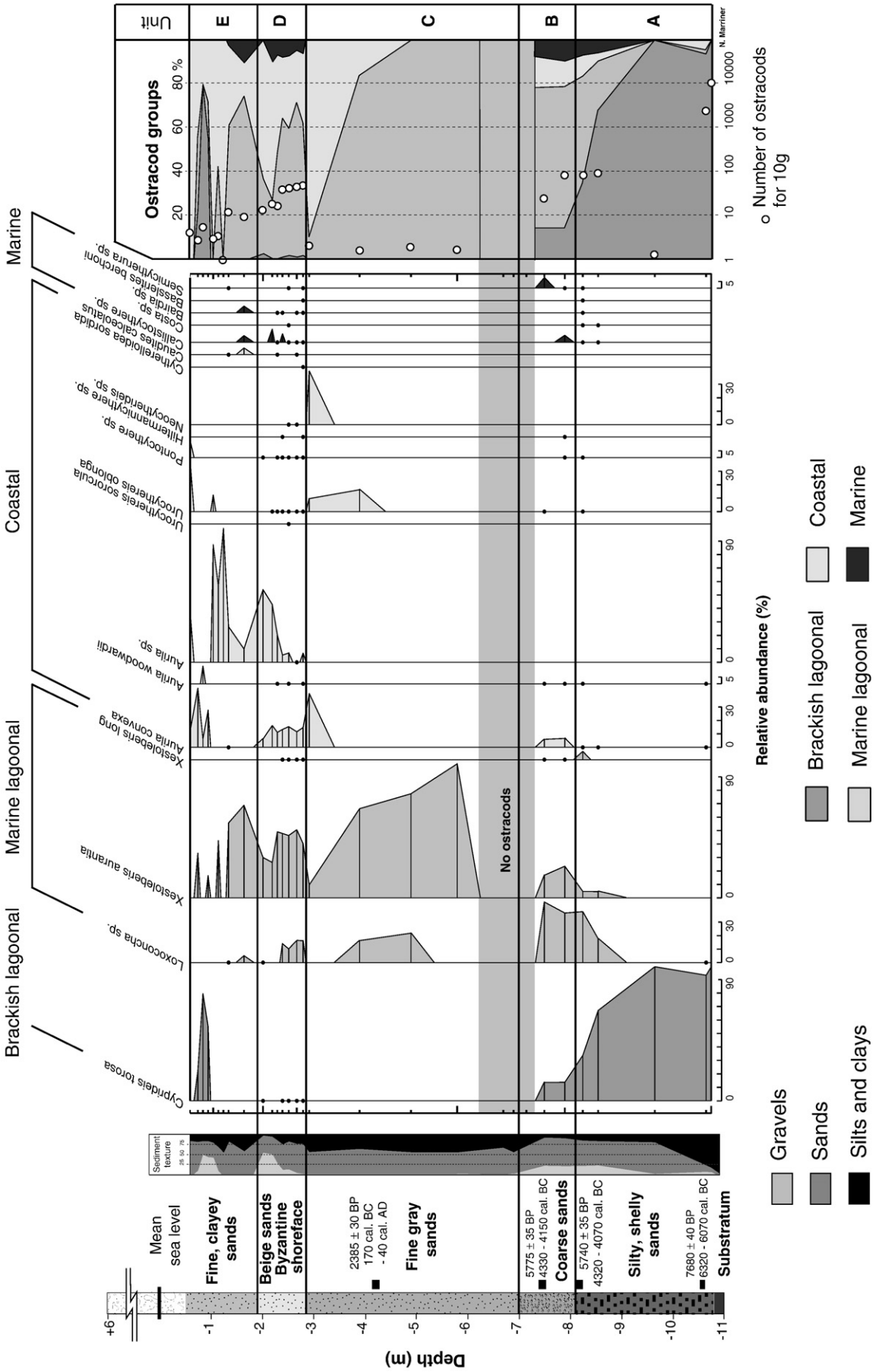

Fig. 12. Core T15 ostracods.

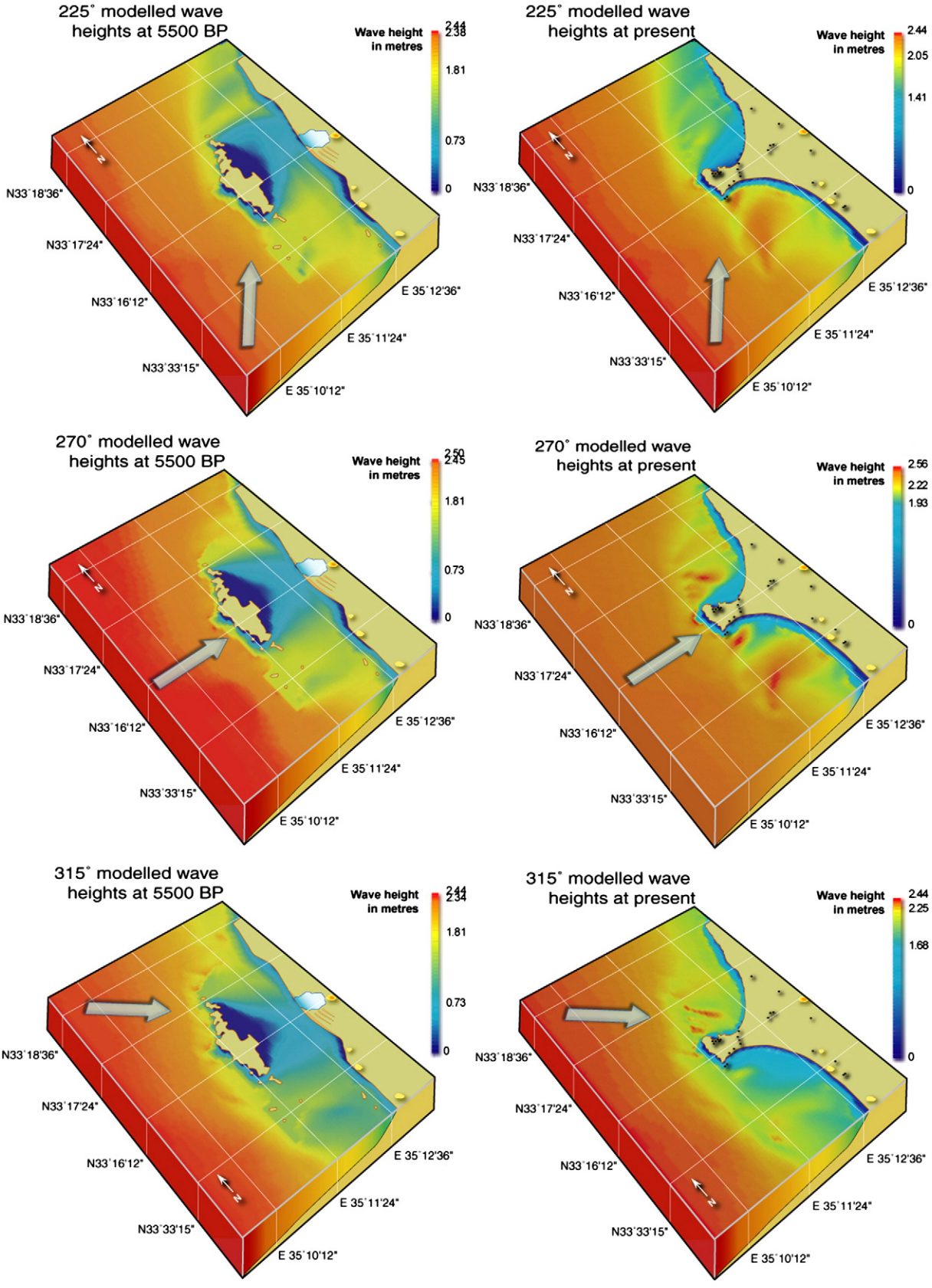

Fig. 13. Wave heights for 225°, 270° and 315° propagated swells (adapted from Marriner et al., 2007).

Holocene marine bottom, leeward of the island breakwater and akin to a stratigraphic trap; (2) formation of a wave-dominated proto-tombolo after 6000 BP; and (3) the wide-reaching anthropogenic impacts of the Hellenistic causeway (Fig. 14).

5.1.1. Origin and development — Early Holocene transgression (8000 to 6000 cal. years BP)

A north–south transect comprising three cores, T13, T14 and T15, elucidates the tombolo's stratigraphy. In this area, leeward of the island breakwater, the Maximum Flooding Surface (MFS) is dated to ~8000 BP (Fig. 15). The litho- and biostratigraphic signatures of this transgression comprise silt and sand rich in molluscan shells. Fine-grained sediments and brackish and marine-lagoonal faunas translate shallow, low-energy waterbodies during this period. Shelter was afforded by Tyre's elongated sandstone ridges which cumulatively acted as a shore-parallel breakwater, corroborated by the numerical models.

Core T18 was drilled between Tell Mashuk and El Bass, the oldest portion of the continental salient *sensu stricto*. Two contrasting facies record the early growth of the tombolo margin. The clay substratum is transgressed by fine-bedded marine sand dated to ~6000 BP (Figs. 4–5). After 5500 BP, the transition from marine sand to choked lagoon sediments is concurrent with the accretion of the salient, culminating in the isolation of the back-barrier lagoon. This rapid coastal accretion is explained by the mid-Holocene stillstand regime and high sediment supply, inducing a loss of accommodation space. Although the density of core networks does not allow the precise spatial dimensions of the lagoon to be established, local

Inset 1: Reconstructed island dimensions around 8000 BP. The bathymetry has been calculated on the basis of a 7 m RSL change.

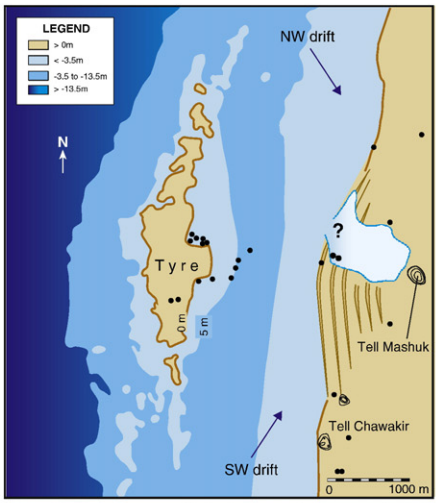

Inset 3: Reconstructed island dimensions around 4000 BP. The bathymetry has been calculated on the basis of a 4.5 m RSL change.

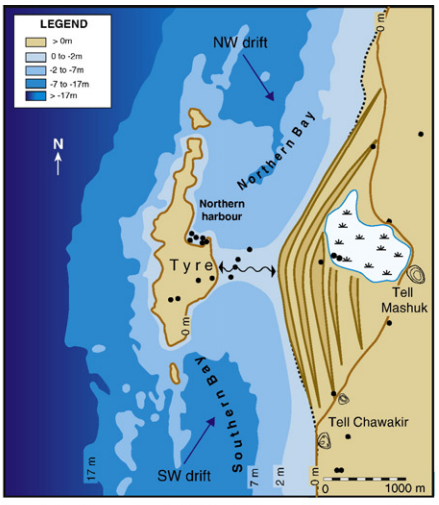

Inset 5: Reconstructed island dimensions around 330 BC. The bathymetry has been calculated on the basis of a 3 m RSL change.

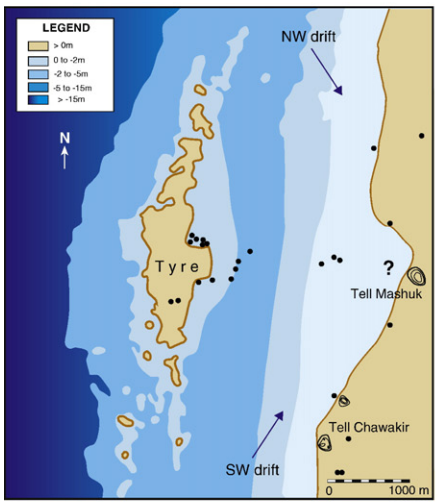

Inset 2: Reconstructed island dimensions around 6000 BP and maximum marine ingression. The bathymetry has been calculated on the basis of a 5 m RSL change.

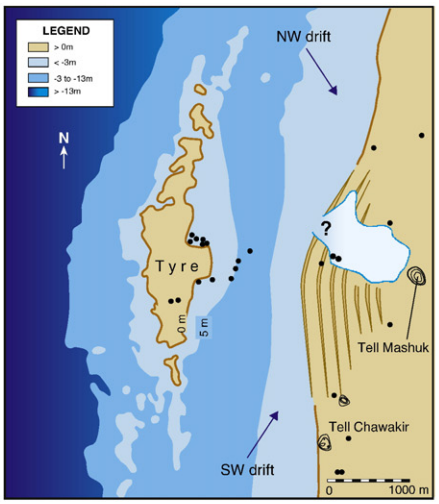

Inset 4: Reconstructed island dimensions around 3000 BP. The bathymetry has been calculated on the basis of a 4 m RSL change.

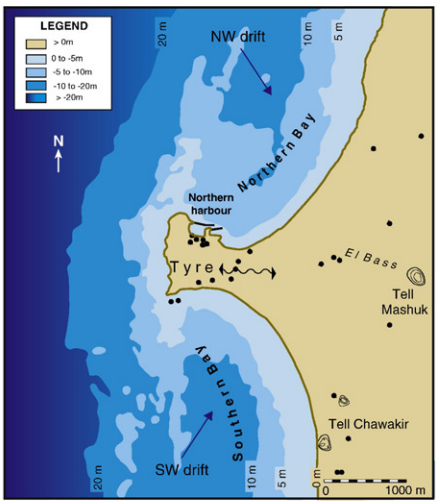

Inset 6: Present day coastal morphology and bathymetry

Fig. 14. Morphodynamic evolution of Tyre's tombolo between ~8000 BP and today. Bathymetric data were derived from the 1998 SHOM marine map of the Tyrian coastal area (Service Hydrographique et Océanographique de la Marine, 1998, Ports du Liban, 7514, 1:25000) and coupled with our chronostratigraphic datasets to obtain a representative coastal reconstruction of Tyre at each time slice.

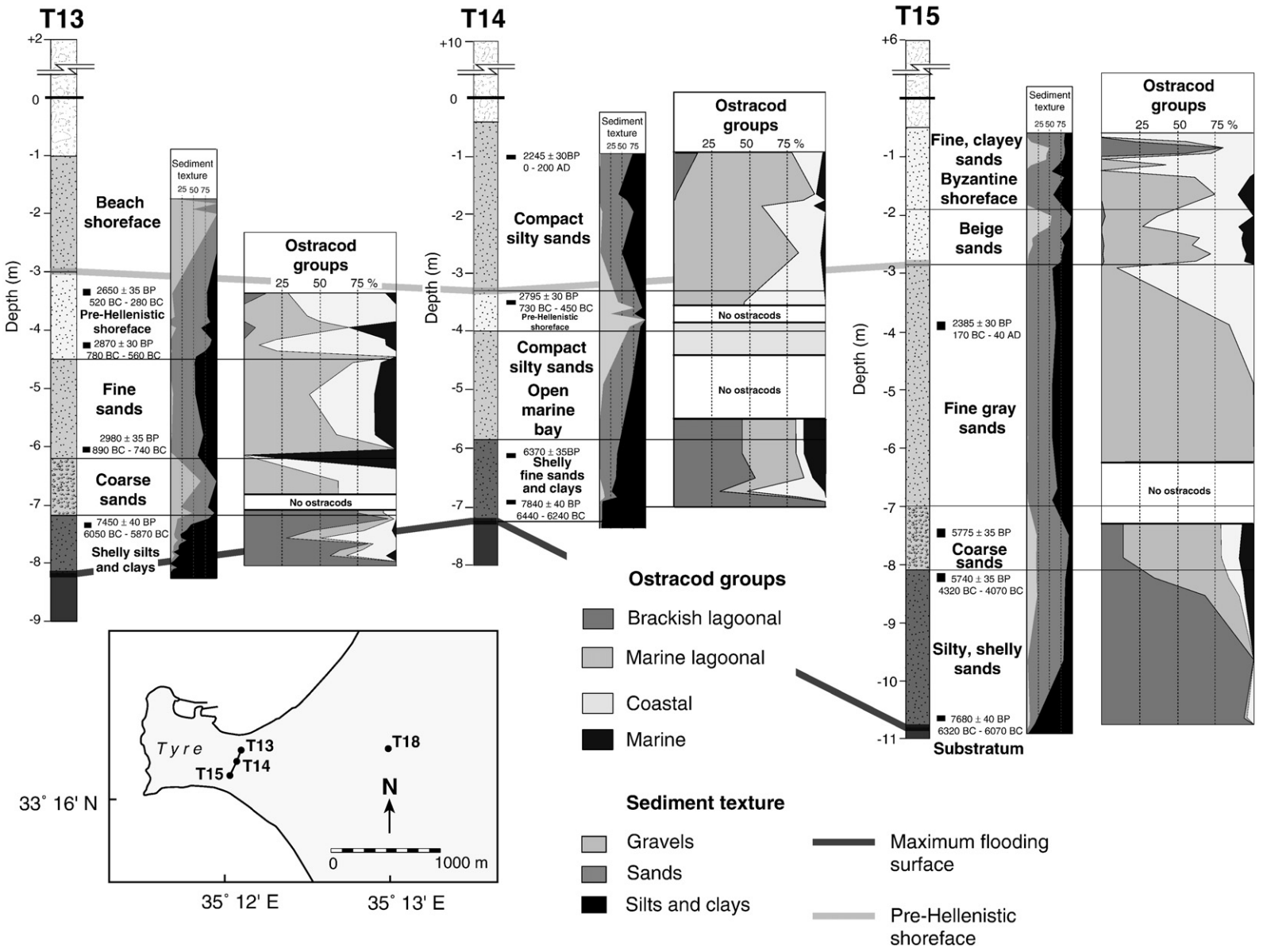

Fig. 15. Chrono- and ostracod biostratigraphy of tombolo cores T13–T15.

topography and geomorphological prospections in this area suggest that at its greatest extent, it could have reached the base of Tell Mashuk, a Bronze Age settlement presently landlocked ~1700 m from the sea (Marriner et al., in press).

Stratigraphies north and south of this lagoon system have yielded prograding ridge systems. Core T7 shows that the base of Tell Chawakir was transgressed before rapidly prograding to form the southern continental base of the salient. Between Tell Chawakir and Tell Rachidiye, the stratigraphy has revealed a series of Pleistocene paleosols similar to those encountered on the Carmel coast (Cohen-Seffer et al., 2005). No marine deposits have been elucidated in this area, pertaining to the relative stability of this portion of Tyre's maritime façade during the Holocene.

5.1.2. Pre-Hellenistic proto-tombolo phase (6000 to 2400 cal. years BP)

After 6000 BP, Tyre's leeward bay was transgressed by coarse sand and gravel deposits. A sharp decline in *C. torosa* is countered by peaks of coastal ostracod species, consistent with an important opening-up of the environment. Our data suggest that sea-level stillstand after 6000 BP was the biggest single factor in the initial development of Tyre's tombolo (Fig. 16).

After 3000 BP, the chronostratigraphic data provide evidence of very rapid rates of sedimentation, >0.3 cm/year (Fig. 17). We link this to human-induced erosion of surrounding watersheds, namely the expansion of agriculture and deforestation, which delivered increased sediment supply to coastal depocentres. Climate records from the Levantine basin evoke a transition to a cool wet climate during the Late Bronze Age/Early Iron Age and the Late Roman/Byzantine periods (Bar-Matthews et al., 1997; Schilman et al., 2001; Enzel et al., 2003; McGarry et al., 2004).

During Hellenistic times Tyre island had approximate dimensions of ~2500 m long by ~750 m wide, flanked to the east by a natural sand bank 1–2 m below MSL (Marriner et al., 2007). Sunamura and Mizuzo (1987) have calculated that a tombolo forms where the ratio of the island's offshore distance to its length is equal or less than 1.5; a salient forms where it is 1.5–3.5, and no protrusion of the coast occurs where it is greater than 3.5. At Tyre, the present ratio is 1.47, at the very limit for tombolo formation. During the Iron Age, however, this ratio was much lower, for example 0.55, consistent with an elongated island in close proximity to the adjacent shoreline (Marriner et al., 2007, in press; Fig. 14). The large discrepancies are notably due to tectonic collapse of the island bastion during the late Roman period (Morhange et al., 2006; Elias et al., 2007), with a reduction in size of the breakwater island by ~50% (Marriner, 2007). Wave diffraction and a fall in water competence led to the deposition of a medium to fine-grained sediment on the lee of the island barrier. The modelling data corroborate conditions conducive to the accretion of this sub-littoral sand bank (Fig. 13), critical to the construction of Alexander's causeway.

5.1.3. Anthropogenic forcing — causeway impacts

The Hellenistic causeway led to a human-induced metamorphosis of Tyre's coastal system accentuating many of the proto-tombolo genetic processes. After ~330 BC, the city's bays were definitively segmented into two coves characterised by two isolated littoral cells. A cessation of longshore currents is linked to human impacts and subaerial growth of the isthmus. During

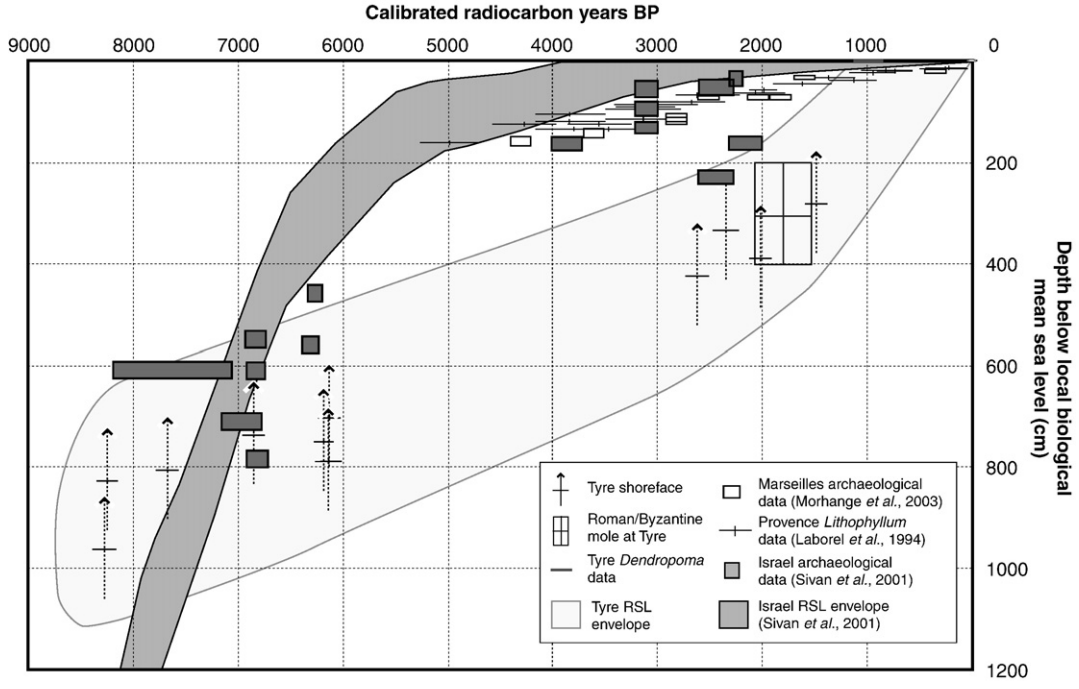

Fig. 16. Sea-level tendencies at Tyre since 8000 BP.

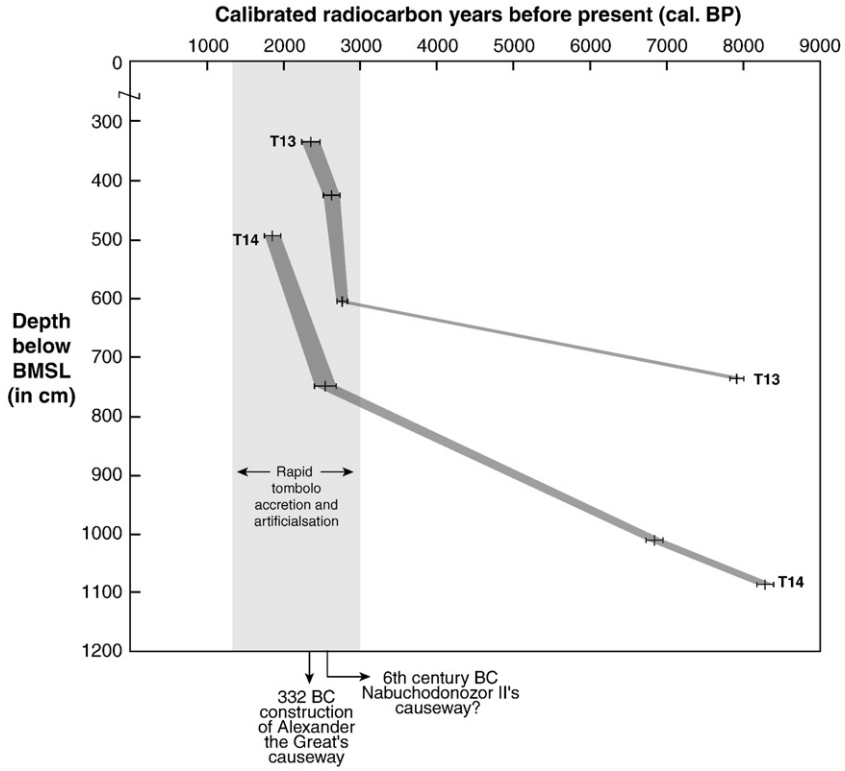

Fig. 17. Tombolo sedimentation rates from cores T13 and T14.

Roman times, this progradation accommodated urban growth (necropolis, hippodrome etc.).

5.1.4. Holocene sea-level tendencies at Tyre

Holocene sea-level tendencies at Tyre are depicted in Fig. 16. Although the results fit well with low error (±5 cm) sea-level data from the stable coasts of Provence (Laborel et al., 1994; Morhange et al., 2001, 2003), the large error margins and absence of accurate sea-level indicators found at Tyre mean that the envelope cannot be used as a precise RSL curve. The 3 m collapse of the Tyrian horst during the late Roman period is evidenced by two types of data (i) Archaeological — Tyre's northern Roman mole is currently 2.5 m below present sea level (Descamps, personal communication), translating a subsidence of ~3–3.5 m. On the southern shore, walls and drowned quarries at −2.5 m below MSL have also been discovered (El Amouri et al., 2005); and (ii) Stratigraphic — similar subsidence is translated in the city's coastal stratigraphy, notably a ~3 m offset in sediment accommodation space and radiocarbon dated strata between Tyre and Sidon (Marriner, 2007).

5.2. Tyre vs. Alexandria: forcing agents and geomorphology

One of the most celebrated tombolo examples, both in terms of its geological and archaeological scopes, is that of Alexandria ad Aegyptum (Goiran, 2001; Goiran et al., 2005). The palaeo-island of Pharos is today a heavily urbanised peninsula, 3.25 long by 1.1 km wide, linked to the continent by a 1.3×0.7 km isthmus (Fig. 17). The tombolo separates two marine bays: a 2×1.5 km eastern bay (Stanley and Bernasconi, 2006), which sheltered a series of seaport complexes during antiquity, and a large western bay (10 km long by 2.5 km wide) partially protected by the drowned extension of the Pharos aeolianite ridge. The presence of this offshore ridge has significantly influenced swell currents on its leeward side. Both bays today operate as isolated littoral cells whilst offshore the dominant marine currents and sediment drift run west to east (Fig. 18).

Geomorphological and chronological parallels between Tyre and Alexandria render a direct comparison of the two sites particularly interesting from a number of aspects. (1) The *geomorphology* of both sites has been significantly influenced by the inherited Pleistocene landscapes, namely a series of partially-drowned aeolianite ridges that run parallel to the present coastline (Butzer, 1962; Stanley and Hamza, 1992; El-Asmar and Wood, 2000) and between which great tracts of Holocene coastal sediments have accumulated. (2) This drowned topography has given rise to *two breakwater islands* (Fig. 19). The dimensions of both breakwaters have changed significantly since their marine flooding between 8000 and 7500 BP. Changes in the size of the shielding breakwaters are discernible in the Holocene sediment record. As at Tyre, ancient Alexandria comprised a long shore-parallel breakwater (Pharos ridge) whose reconstructed Hellenistic dimensions, ~5500 m long by ~1300 m wide, are approximately twice those at Tyre for the same period (Goiran, 2001). (3) Both sites lie in *proximity to important fluvial systems*, the Nile (Said, 1993) and the Litani (Abd-el-Al, 1948). Although the scales of these fluvial systems are not directly comparable, the two rivers were significant in dictating sediment budgets and the nature of the highstand deposits during the accretion of the tombolos (Chen et al., 1992; Warne and Stanley, 1993a,b; Stanley and Warne,

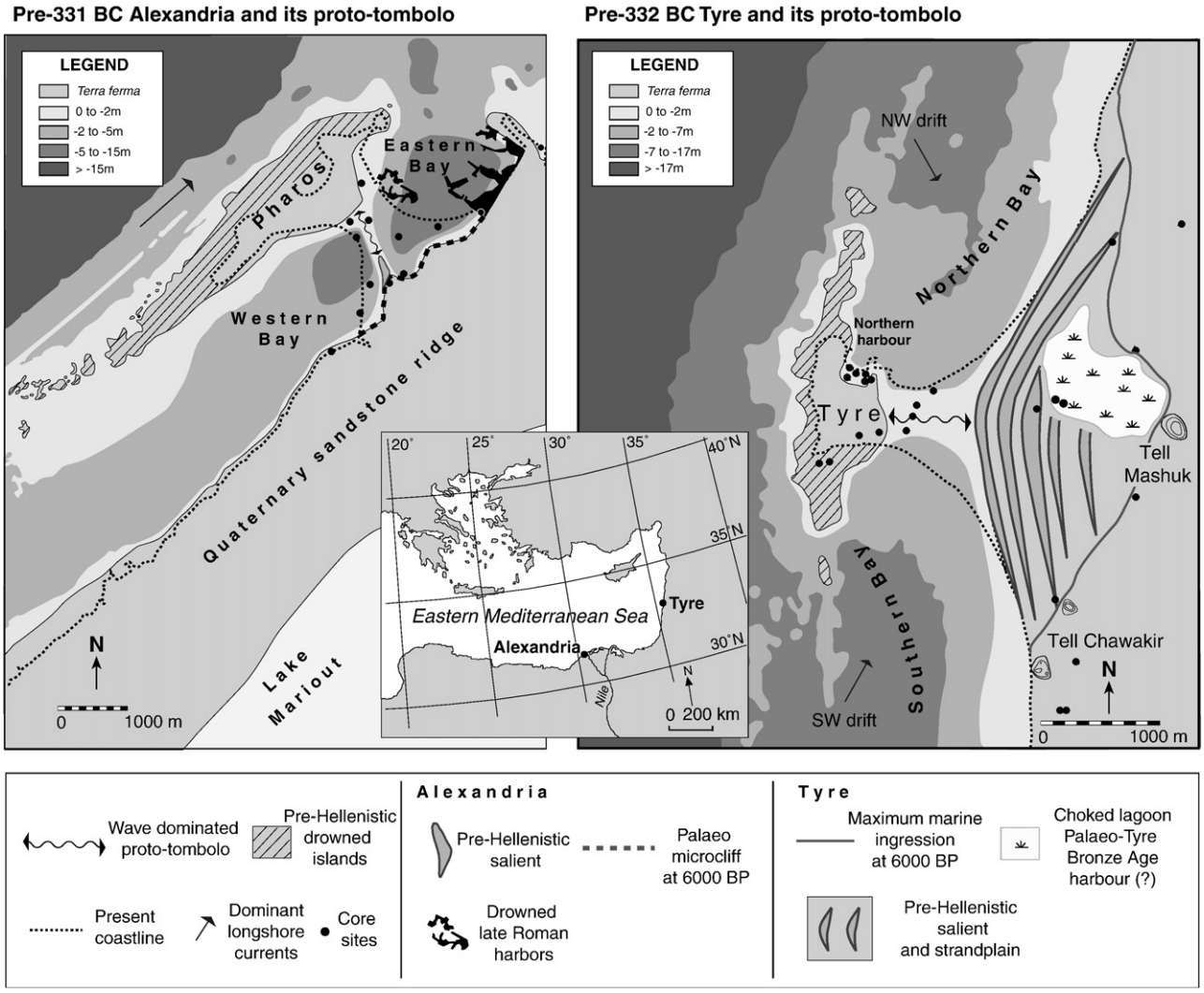

Fig. 18. Morphodynamic evolution of the Alexandria and Tyre isthmuses since antiquity.

1998). (4) Alexandria and Tyre were modified by *human intervention* at the same time (332 and 331 BC). Assessing the synchronicity or disynchronicity of stratigraphic impacts is interesting from geomorphological and historical perspectives. (5) The two sites underwent significant *subsidence around the late Roman period* (~6±0.5 m at Alexandria and ~3±0.5 m at Tyre). These rapid relative sea-level movements had two impacts: (a) from a geomorphological standpoint, it greatly diminished the dimensions of the breakwater obstacles, reducing the size of the wave shadows; and (b) from a stratigraphic perspective, it created significant accommodation space for the deposition of new sediment tracts.

5.3. Description and interpretation of the tombolo stratigraphy at Alexandria

On the basis of a 10 m-long transgressive–regressive sediment sequence (C2; Goiran, 2001) a series of phases in the accretion of Alexandria's tombolo have been elucidated (Fig. 19). The proximity of core C2 to the Heptastadium renders it particularly sensitive in recording geomorphological changes and human impacts. We note a number of stratigraphic similarities between Alexandria and Tyre.

5.3.1. Phase 1 — marine flooding (8000 to 6000 cal. years BP)

Like Tyre, the inception of marine sedimentation at Alexandria is dated to ~7800 BP, consistent with the flooding of deltas throughout the circum-Mediterranean (Stanley and Warne, 1994). This flooding surface is onlapped by a shelly sand unit coeval with the reworking of transgressed deposits.

5.3.2. Phase 2 — accretion of the proto-tombolo (6000 to 2400 cal. years BP)

Between 5400 BP and 4200 BP, we elucidate a *Cladocora* biodeposition in cores C2 and C9, comprising broken coral branches enveloped in a silty clay matrix (Fig. 19). The chronostratigraphic analogue at Tyre constitutes medium-grained sand. The origin of this biodeposition is explained by the erosion of bioherms in proximity to Alexandria. Juxtaposition of coarse and fine-grained sediment stocks evokes seasonality in currents and sediment deposition patterns; the coarse biodeposition is inferred to have been reworked and deposited during winter

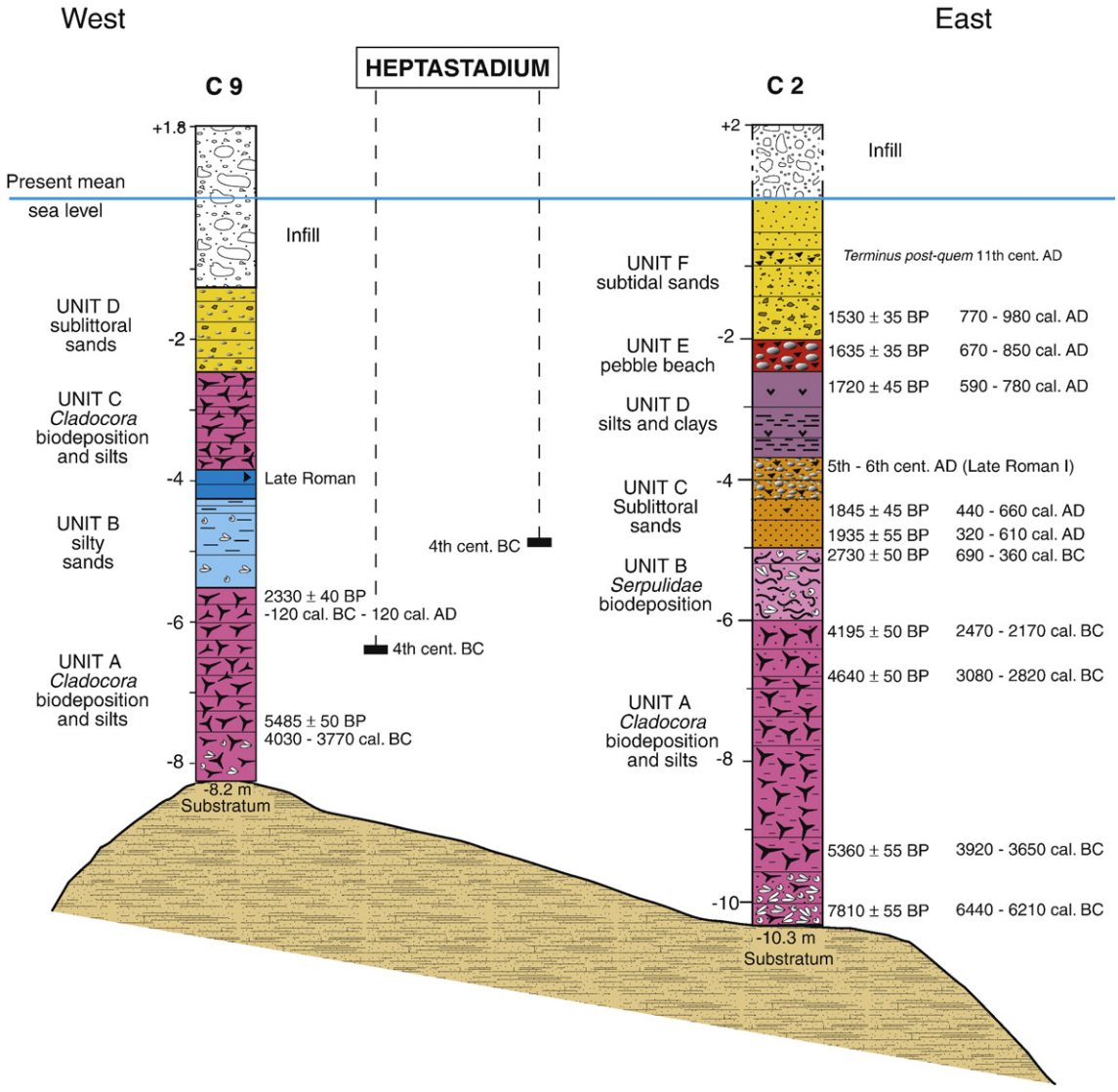

Fig. 19. Chronostratigraphy of tombolo cores C9 and C2 at Alexandria.

storms, subsequently enveloped in a silt–clay matrix during Nile summer flooding (Goiran, 2001). 95% of the ostracod fauna is dominated by the marine-lagoonal species *Xestoleberis* sp. and *Loxoconcha* sp. Secondary taxa include the coastal species *Urocythereis* sp. and *A. convexa*. This evokes a medium to low-energy environment protected by the partially-drowned ridge system. Using topographic and bathymetric data we have reconstructed the palaeogeography of Alexandria at 5500 BP, underlining the importance of the subaerial ridge in protecting the site's western bay. The ridge formed a barrier over 14 km long stretching from the eastern tip of Pharos westwards towards the Agami promontory (Fig. 20). These litho- and biostratigraphic findings support data from Tyre, characterised by marine-lagoonal fauna and a medium to low-energy sedimentology. By contrast, the lateral extension of Tyre's semi-drowned ridge (4 km) was greatly inferior to Alexandria (14 km) between 6000 BP and 4000 BP.

A sediment hiatus is recorded between 4000 BP and 2000 BP, a time period that straddles the construction of Alexander's causeway. A fall in sediment supply is improbable given the rapid and synchronous progradation of the Nile delta at this time (Warne and Stanley, 1993a,b; Stanley and Warne, 1998). We suggest that significant portions of the Pharos ridge were drowned and breached after 4000 BP (Fig. 20). The subsequent creation of more powerful westerly currents could be at the origin of non-deposition of parts of the proto-tombolo. At this time, Stanley and Bernasconi (2006) have described an open marine environment inside the eastern bay. Faced with this problem, the Romans constructed artificial marinas in this area (Goddio et al., 1998; Goddio and Bernand, 2004; Bernasconi et al., 2006). After 2085±45 ^{14}C BP (200 to 410 cal. AD), a *Serpulidae* biodeposition corroborates the dynamic marine currents following the construction of the Heptastadium causeway.

5.3.3. Phase 3 — human and tectonic impacts (after 2400 cal. years BP)

5.3.3.1. Subaerial progradation phase 1. Progradation of the tombolo is indicated by the accretion of a sand unit after 1935± 55 ^{14}C BP (360 to 610 cal. AD). The molluscan macrofauna

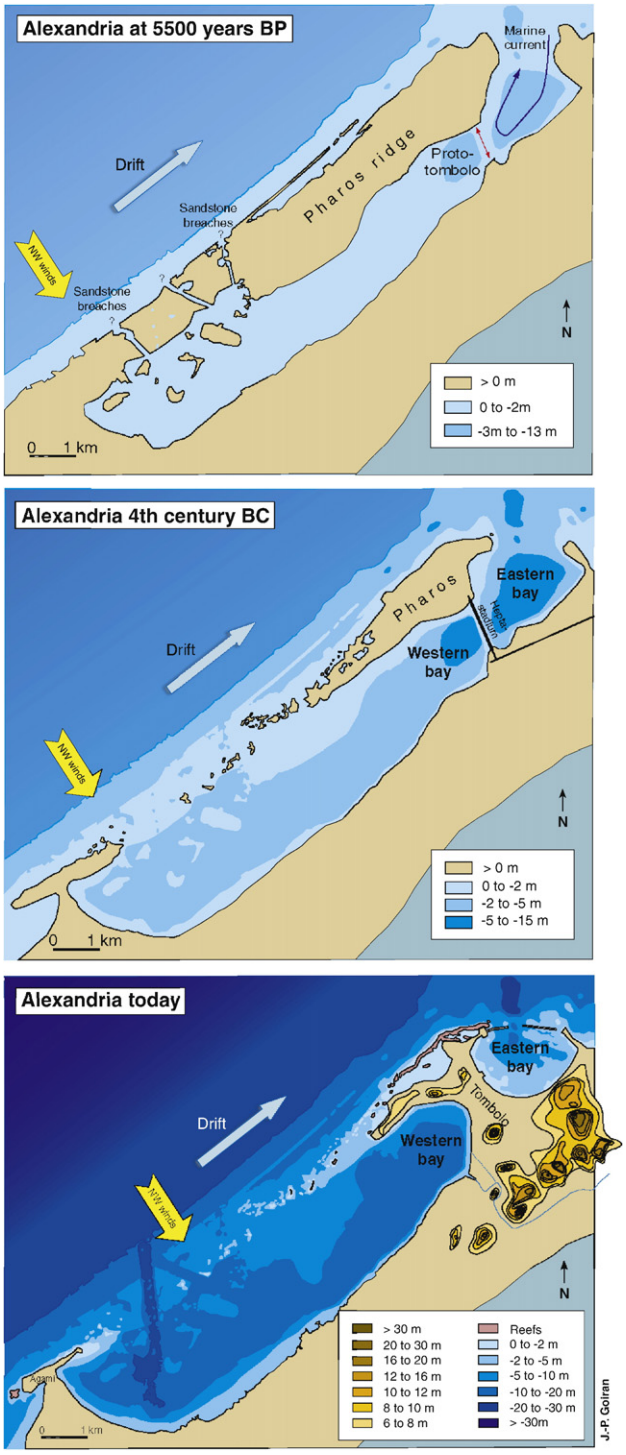

Fig. 20. Top: Palaeogeographical reconstruction of Alexandria's tombolo around 5500 BP. The reconstruction factors in a relative sea-level change of 7 m since this time. Note the existence of an extensive 14 km breakwater ridge that shielded Alexandria's western bay. We hypothesise that a number of breaches existed in the sandstone ridge creating a low-energy lagoon environment on the leeward side at this time. Middle and bottom: Palaeogeographical reconstruction of Alexandria's tombolo at 330 BC. The reconstruction factors in a 5 m relative sea-level change since the Ptolemaic period that has significantly reduced the dimensions of Pharos island.

is dominated by three assemblages: the upper clean-sand assemblage (*Cyclope donovani*, *Sphoeronassa mutabilis*, *Spisula subtruncata*, *Venus gallina*), the upper muddy-sand assemblage in sheltered areas (*Venerupis rhomboides*), and the sublittoral sands assemblage (*B. reticulatum latreilli*, *R. lineolata*). The ostracod fauna is dominated by lagoonal (65% of the relative abundance) and coastal taxa (30%). The litho- and biostratigraphies concur progradation of the salient flanks, with its passage from a marine to continental form characterised by wide sandy beaches.

5.3.3.2. Tectonic collapse. During the 7th–9th centuries AD, tectonic collapse accounts for the rapid submersion of great tracts of the tombolo (Goiran, 2001; Goddio et al., 2006). Recent underwater archaeological research undertaken on the western margin of the Nile delta (embouchure of the Canopic branch and the ancient eastern harbour of Alexandria; Goddio et al., 2006) demonstrates the anomalous presence of late 7th century AD remains at 6 m below present sea level (Goddio et al., 2006), consistent with a collapse of Alexandria's eastern harbour during the 8th century AD (Goiran, 2001). At the same period, the late Roman cities of Eastern Canopus and Herakleion experienced a similar catastrophic event. Regional instability has been linked to substantial readjustment of the 5000 m-thick Tertiary and Quaternary Nile sediments (Said, 1993).

This 6 m collapse generated considerable accommodation space and led to the deposition of a diverse sedimentary facies, consistent with anthropogenic impacts. Most of the cores attest to coarse sediments except inside the renovated harbour basins where silt facies are indicative of artificial confinement. For example, in C2, silt deposits and gypsum crystals are consistent with a low-energy environment, indicative of an artificial harbour basin.

5.3.3.3. Subaerial progradation phase 2. The coastal response of this catastrophic submersion was rapid as the tombolo established a new equilibrium profile in balance with the high local sediment budget. After 1635±35 ^{14}C BP (8th–9th centuries AD), transition to a rounded pebble then coarse sand facies corroborates the progradation of the tombolo flanks, accelerated by the creation of new accommodation space. Rapid coastal deformation during the Islamic and Medieval periods is concurrent with data from Tyre, and is typical of semi-open environments with a high sediment budget.

6. Conclusions

Largely concomitant chronostratigraphies at Tyre and Alexandria attest to the importance of the offshore island breakwaters in creating pre-Hellenistic proto-tombolos. Our data indicate that the salients lay within 1–2 m of sea level by the time of Alexander the Great, thus considerably facilitating the construction of Alexander's causeways. At both sites, the causeway impacts are quasi-identical, with the irreversible segmentation of the original bays coupled with a sharp fall in water competence, leading to a complete human-induced metamorphosis of the Tyrian and Alexandrian coastal systems. Finally, the study demonstrates

the scope of an applied geomorphological approach in helping to answer archaeological questions.

Acknowledgements

The authors wish to thank the ANR-CNRS (GEOPAM), the Association Internationale pour la Sauvegarde de Tyr, CEAlex UMS 1218, the Supreme Council of Archaeology in Egypt, the head of Islamic Antiquity, the Lebanese Directorate General of Antiquities, the Franco-Lebanese program Cèdre, ECLIPSE/CNRS, UNESCO CPM and the Leverhulme Trust for technical and financial support. This research is a contribution to the project ArcheoMed: patrimoine culturel de la Méditerranée (InterReg IIIB MEDOCC).

References

Abd-el-Al, I., 1948. Le Litani, étude hydrologique. Service hydrologique de la République Libanaise, Beirut.

Anthony, E.J., Blivi, A.B., 1999. Morphosedimentary evolution of a delta-sourced, drift-aligned sand barrier–lagoon complex, western Bight of Benin. Marine Geology 158, 161–176.

Barash, A., Danin, Z., 1992. Fauna Palaestina, mollusca I. Annotated List of Mediterranean Molluscs of Israel and Sinai. The Israel Academy of Sciences and Humanities, Jerusalem.

Bar-Matthews, M., Ayalon, A., Kaufman, A., 1997. Late Quaternary paleoclimate in the Eastern Mediterranean Region from stable isotope analysis of speleothems in Soreq cave, Israel. Quaternary Research 47, 155–168.

Bellan-Santini, D., Lacaze, J.C., Poizat, C., 1994. Les biocénoses marines et littorales de Méditerranée. Coll. Patrimoines Naturels, vol. 19. Muséum National d'Histoire Naturelle.

Bernasconi, M.P., Melis, R., Stanley, J.-D., 2006. Benthic biofacies to interpret Holocene environmental changes and human impact in Alexandria's Eastern Harbour, Egypt. Holocene 16, 1163–1176.

Bitar, G., Kouli-Bitar, S., 1998. Inventaire des mollusques marines benthiques du Liban et remarques biogéographiques sur quelques espèces nouvellement signalés. Mesogée 56, 37–44.

Blanc, J.-J., 1959. Recherches sédimentologiques littorales et sous-marines en Provence occidentale, PhD thesis. Masson, Paris.

Blivi, A., Anthony, E.J., Oyédé, L.M., 2002. Sand barrier development in the bight of Benin, West Africa. Ocean and Coastal Management 45, 185–200.

Bronk Ramsey, C., 2001. Development of the radiocarbon program OxCal. Radiocarbon 43, 355–363.

Browder, A.G., McNinch, J.E., 2006. Linking framework geology and nearshore morphology: correlation of paleo-channels with shore-oblique sandbars and gravel outcrops. Marine Geology 231, 141–162.

Butzer, K.W., 1962. Pleistocene stratigraphy and prehistory in Egypt. Quaternaria 6, 451–477.

Carmel, Z., Inman, D.L., Golik, A., 1985a. Characteristics of storm waves off the Mediterranean coast of Israel. Coastal Engineering 9, 1–19.

Carmel, Z., Inman, D.L., Golik, A., 1985b. Directional wave measurement at Haifa, Israel, and sediment transport along the Nile littoral cell. Coastal Engineering 9, 21–36.

Carmona, P., Ruiz, J.M., 2004. Geomorphological and geoarchaeological evolution of the coastline of the Tyre tombolo: preliminary results. Bulletin d'Archéologie et d'Architecture Libanaises Hors-Série 1, 207–219.

Cattaneo, A., Steel, R.J., 2003. Transgressive deposits: a review of their variability. Earth-Science Reviews 62, 187–228.

Catuneanu, O., 2002. Sequence stratigraphy of clastic systems: concepts, merits, and pitfalls. Journal of African Earth Sciences 35, 1–43.

Catuneanu, O., 2005. Principles of Sequence Stratigraphy. Elsevier, London.

Chen, Z., Warne, A.G., Stanley, D.J., 1992. Late Quaternary evolution of the northwestern Nile Delta between Rosetta and Alexandria, Egypt. Journal of Coastal Research 8, 527–561.

Clemmensen, L.B., Richardt, N., Andersen, C., 2001. Holocene sea-level variation and spit development: data from Skagen Odde, Denmark. Holocene 11, 323–331.

Cohen-Seffer, R., Greenbaum, N., Sivan, D., Jull, T., Barmeir, E., Croitoru, S., Inbar, M., 2005. Late Pleistocene-Holocene marsh episodes along the Carmel coast, Israel. Quaternary International 140−141, 103–120.

Courtaud, J., 2000. Dynamiques géomorphologiques et risques littoraux. Cas du Tombolo de Giens (Var, France méridionale), PhD thesis. Université de Provence, Aix-en-Provence.

Dally, W.R., Pope, J., 1986. Detached breakwaters for shore protection. Technical Report. Coastal Engineering Research Centre, Waterways Experiment Station. CERC-86-1.

Davies, J.L., 1980. Geographical Variation in Coastal Development. Longman, London.

Davis, R.A. (Ed.), 1994. Geology of Holocene Barrier Island Systems. Springer-Verlag, Berlin.

Doneddu, M., Trainito, E., 2005. Conchiglie del Mediterraneo. Il Castello, Trezzano sul Naviglio.

Doumet-Serhal, C. (Ed.), 2004. Decade: a decade of archaeology and history in the Lebanon. Archaeology and History in Lebanon, Beirut.

Dubertret, L., 1955. Carte géologique du Liban au 1:200,000, avec notice explicative. Ministère des Travaux Publics, Beyrouth.

El Amouri, M., El Helou, M., Marquet, M., Noureddine, I., Seco Alvarez, M., 2005. Mission d'expertise archéologique du port sud de Tyr, sud Liban: résultats préliminaires. Bulletin d'Archéologie et d'Architecture Libanaises. Hors-Série, vol. 2, pp. 91–110.

El-Asmar, H.M., Wood, P., 2000. Quaternary shoreline development: the northwestern coast of Egypt. Quaternary Science Reviews 19, 1137–1149.

Elias, A., Tapponnier, P., Singh, S.C., King, G.C.P., Briais, A., Daëron, M., Carton, H., Sursock, A., Jacques, E., Jomaa, R., Klinger, Y., 2007. Active thrusting offshore Mount Lebanon: source of the tsunamigenic A.D. 551 Beirut–Tripoli earthquake. Geology 35, 755–758.

Enzel, Y., Bookman, R., Sharon, D., Gvirtzman, H., Dayan, U., Ziv, B., Steinc, M., 2003. Late Holocene climates of the Near East deduced from Dead Sea level variations and modern regional winter rainfall. Quaternary Research 60, 263–273.

Escoffier, F.F., 1954. Travelling forelands and the shoreline processes associated with them. Bulletin US Beach Erosion Board 9, 11–14.

Fleming, W.B., 1915. History of Tyre. Columbia University Press, New York.

Flinn, D., 1997. The role of wave diffraction in the formation of St. Ninian's Ayre (Tombolo) in Shetland, Scotland. Journal of Coastal Research 13, 202–208.

Frechen, M., Dermann, B., Boenigk, W., Ronen, A., 2001. Luminescence chronology of aeolianites from the section at Givat Olga — Coastal Plain of Israel. Quaternary Science Reviews 20, 805–809.

Frechen, M., Neber, A., Dermann, B., Tsatskin, A., Boenigk, W., Ronen, A., 2002. Chronostratigraphy of aeolianites from the Sharon Coastal Plain of Israel. Quaternary International 89, 31–44.

Frechen, M., Neber, A., Tsatskin, A., Boenigk, W., Ronen, A., 2004. Chronology of Pleistocene sedimentary cycles in the Carmel Coastal Plain of Israel. Quaternary International 121, 41–52.

Gardner, J.V., Dartnell, P., Mayer, L.A., Hughes Clarke, J.E., Calder, B.R., Duffy, G., 2005. Shelf-edge deltas and drowned barrier-island complexes on the northwest Florida outer continental shelf. Geomorphology 64, 133–166.

Goddio, F., Bernand, A., 2004. Sunken Egypt — Alexandria. Periplus, London.

Goddio, F., Bernand, A., Bernand, E., Darwish, I., Kiss, Z., Yoyotte, J., 1998. Alexandria: the Submerged Royal Quarters. Periplus, London.

Goddio, F., Clauss, M., Gerigk, C., 2006. Egypt's Sunken Treasures. Prestel Publishing, London.

Goiran, J.-P., 2001. Recherches géomorphologiques dans la région littorale d'Alexandrie, Egypte, PhD thesis. Université de Provence, Aix-en-Provence.

Goiran, J.-P., Marriner, N., Morhange, C., Abd El-Maguib, M., Espic, K., Bourcier, M., Carbonel, P., 2005. Evolution géomorphologique de la façade maritime d'Alexandrie (Egypte) au cours des six derniers millénaires. Méditerranée 104, 61–64.

Goldsmith, V., Sofer, S., 1983. Wave climatology of the southeastern Mediterranean. Israel Journal of Earth Science 32, 1–51.

Gosseaume, E., 1973. Le tombolo triple d'Orbetello (Toscane). Bulletin de la Société Languedocienne de Géographie 7, 3–11.
Guilcher, A., 1958. Coastal and Submarine Morphology. Methuen and Co. Ltd., London.
Gulliver, F.P., 1896. Cuspate forelands. Geological Society of America Bulletin 7, 399–422.
Gulliver, F.P., 1899. Shoreline topography. Proceedings of the American Academy of Arts and Science 34, 149–258.
Hesse, A., 1998. Arguments pour une nouvelle hypothèse de localisation de l'Heptastade d'Alexandrie. Etudes alexandrines 1, 1–33.
Hine, A.C., 1979. Mechanisms of berm development and resulting beach growth along a barrier spit complex. Sedimentology 6, 333–351.
Johnson, D.W., 1919. Shore Processes and Shoreline Development. Wiley, New York.
Katzenstein, H.J., 1997. The History of Tyre. Ben-Gurion University of the Negev Press, Jerusalem.
Laborel, J., Laborel-Deguen, F., 1994. Biological indicators of relative sea-level variations and co-seismic displacements in the Mediterranean region. Journal of Coastal Research 10, 395–415.
Laborel, J., Morhange, C., Lafont, R., Le Campion, J., Laborel-Deguen, F., Sartoretto, S., 1994. Biological evidence of sea-level rise during the last 4500 years on the rocky coasts of continental southwestern France and Corsica. Marine Geology 120, 203–223.
Marriner, N., 2007. Geoarchaeology of Phoenicia's buried harbours: Beirut, Sidon and Tyre: 5000 years of human–environment interactions, unpublished PhD thesis. Université de Provence, Aix-en-Provence.
Marriner, N., Morhange, C., Doumet-Serhal, C., Carbonel, P., 2006. Geoscience rediscovers Phoenicia's buried harbors. Geology 34, 1–4.
Marriner, N., Morhange, C., Meulé, S., 2007. Holocene morphogenesis of Alexander the Great's isthmus at Tyre in Lebanon. Proceedings of the National Academy of Sciences 104 (22), 9218–9223.
Marriner, N., Morhange, C., Carayon, N., in press. Ancient Tyre and its harbours: 5000 years of human–environment interactions. Journal of Archaeological Science. doi:10.1016/j.jas.2007.09.003.
McGarry, S., Bar-Matthews, M., Matthews, A., Vaks, A., Schilman, B., Ayalon, A., 2004. Constraints on hydrological and paleotemperature variations in the Eastern Mediterranean region in the last 140 ka given by the δD values of speleothem fluid inclusions. Quaternary Science Reviews 23, 919–934.
McKee Smith, J., Sherlock, A.R., Donald, T., 2001. STWAVE: Steady-State Spectral Wave Model User's Manual for STWAVE Version 3.0. U.S. Army Corps of Engineers, Washington DC.
Ming, D., Chiew, Y.-M., 2000. Shoreline changes behind detached breakwater. Journal of Waterway, Port, Coastal, and Ocean Engineering 63–70 March/April.
Morhange, C., Laborel, J., Hesnard, A., 2001. Changes of relative sea level during the past 5000 years in the ancient harbor of Marseilles, Southern France. Palaeogeography, Palaeoclimatology, Palaeoecology 166, 319–329.
Morhange, C., Blanc, F., Bourcier, M., Carbonel, P., Prone, A., Schmitt-Mercury, S., Vivent, D., Hesnard, A., 2003. Bio-sedimentology of the late Holocene deposits of the ancient harbor of Marseilles (Southern France, Mediterranean sea). Holocene 13, 593–604.
Morhange, C., Pirazzoli, P.A., Marriner, N., Montaggioni, L.F., Nammour, T., 2006. Late Holocene relative sea-level changes in Lebanon, Eastern Mediterranean. Marine Geology 230, 99–114.
Nir, Y., 1996. The city of Tyre, Lebanon and its semi-artificial tombolo. Geoarchaeology 11, 235–250.
Otvos, E.G., 2000. Beach ridges — definitions and significance. Geomorphology 32, 83–108.
Otvos, E.G., Giardino, M.J., 2004. Interlinked barrier chain and delta lobe development, northern Gulf of Mexico. Sedimentary Geology 169, 47–73.
Péres, J.-M., 1982. Major benthic assemblages. In: Kinne, O. (Ed.), Marine Ecology, vol. 5, part 1. Wiley, Chichester, pp. 373–522.
Péres, J.-M., Picard, J., 1964. Nouveau manuel de bionomie benthique de la mer Méditerranée. Rec. Trav. Station Marine Endoume, vol. 31. Marseille.
Poppe, G.T., Goto, Y., 1991. European Seashells, vol. I. Verlag Christa Hemmen, Wiesbaden.
Poppe, G.T., Goto, Y., 1993. European Seashells, vol. II. Verlag Christa Hemmen, Wiesbaden.
Ribes, E., Borschneck, D., Morhange, C., Sandler, A., 2003. Recherche de l'origine des argiles du bassin portuaire antique de Sidon. Archaeology and History in Lebanon 18, 82–94.
Rosen, D., Kit, E., 1981. Evaluation of the wave characteristics at the Mediterranean coast of Israel. Israel Journal of Earth Science 30, 120–134.
Said, R., 1993. The River Nile: Geology, Hydrology and Utilization. Pergamon Press, New York.
Sanderson, P., Eliot, I.G., 1996. Shoreline salients on the coast of Western Australia. Journal of Coastal Research 12, 761–773.
Sanlaville, P., 1977. Étude géomorphologique de la région littorale du Liban. Publications de l'Université Libanaise, Beyrouth.
Schilman, B., Bar-Matthews, M., Almogi-Labin, A., Luz, B., 2001. Global climate instability reflected by Eastern Mediterranean marine records during the late Holocene. Palaeogeography, Palaeoclimatology, Palaeoecology 176, 157–176.
Schwartz, R.K., Birkemeier, W.A., 2004. Sedimentology and morphodynamics of a barrier island shoreface related to engineering concerns, Outer Banks, NC, USA. Marine Geology 211, 215–255.
Silvester, R., Hsu, J.R.C., 1993. Coastal Stabilization: Innovative Concepts. Prentice Hall, New Jersey.
Simms, A.R., Anderson, J.B., Blum, M., 2006. Barrier-island aggradation via inlet migration: Mustang Island, Texas. Sedimentary Geology 187, 105–125.
Sivan, D., Porat, N., 2004. Evidence from luminescence for Late Pleistocene formation of calcareous aeolianite (kurkar) and paleosol (hamra) in the Carmel Coast, Israel. Palaeogeography, Palaeoclimatology, Palaeoecology 211, 95–106.
Sivan, D., Wdowinski, S., Lambeck, K., Galili, E., Raban, A., 2001. Holocene sea-level changes along the Mediterranean coast of Israel, based on archaeological observations and numerical model. Palaeogeography, Palaeoclimatology, Palaeoecology 167, 101–117.
Soffer, A., 1994. The Litani River: fact and fiction. Middle Eastern Studies 30, 963–974.
Stanley, D.J., Hamza, H., 1992. Terrigenous-carbonate sediment interface (Late Quaternary) along the northwestern margin of the Nile Delta. Journal of Coastal Research 8, 153–171.
Stanley, D.J., Warne, A.G., 1994. Worldwide initiation of Holocene marine deltas by deceleration of sea-level rise. Science 265, 228–231.
Stanley, D.J., Warne, A.G., 1998. Nile Delta in its destruction phase. Journal of Coastal Research 14, 794–825.
Stanley, D.J., Bernasconi, M.P., 2006. Holocene depositional patterns and evolution in Alexandria's Eastern Harbor, Egypt. Journal of Coastal Research 22, 283–297.
Stapor, F.W., Stone, G.W., 2004. A new depositional model for the buried 4000 yr BP New Orleans barrier: implications for sea-level fluctuations and onshore transport from a nearshore shelf source. Marine Geology 204, 215–234.
Stone, G.W., Liu, B., Pepper, D.A., Wang, P., 2004. The importance of extratropical and tropical cyclones on the short-term evolution of barrier islands along the northern Gulf of Mexico, USA. Marine Geology 210, 63–78.
Sunamura, T., Mizuzo, O., 1987. A study on depositional shoreline forms behind an island. Annual Report of the Institute of Geosciences, the University of Tsukuba 13, 71–73.
Warne, A.G., Stanley, D.J., 1993a. Late Quaternary evolution of the northwest Nile Delta and adjacent coast in the Alexandria region, Egypt. Journal of Coastal Research 9, 26–64.
Warne, A.G., Stanley, D.J., 1993b. Archaeology to refine Holocene subsidence rates along the Nile Delta Margin, Egypt. Geology 21, 715–718.
Zenkovich, V.P., 1967. Processes of Coastal Development. Oliver and Boyd, London.